Biofuel Research Journal 47 (2025) 2451-2469

Biofuel Research Journal

Journal homepage: www.biofueljournal.com

Original Research Paper

Rewiring *Escherichia coli* central carbon metabolism for the sustainable bioconversion of waste glycerol into biodegradable polyhydroxybutyrate

Jittakan Pachimsawat[1], Takeharu Tsuge[2], Suchada Chanprateep Napathorn[1,3,4,*]

[1]*Program in Biotechnology, Faculty of Science, Chulalongkorn University, Phayathai Road, Patumwan, Bangkok 10330, Thailand.*

[2]*Department of Materials Science and Engineering, Institute of Science Tokyo, 4259 Nagatsuta, Midori-ku, Yokohama 226-8502, Japan.*

[3]*Department of Microbiology, Faculty of Science, Chulalongkorn University, Phayathai Road, Patumwan, Bangkok 10330, Thailand.*

[4]*International Center for Biotechnology, The University of Osaka, Suita, 2-1 Yamadaoka, Suita, Osaka 565-0871, Japan.*

HIGHLIGHTS

- Δ*edd* in *E. coli* led to the accumulation of 93 wt% PHB produced from glucose in 30 h.
- *E. coli* Δ*edd*-pBSK-$CAB_{A\text{-}04}$ achieved 7.6 g/L PHB with a 0.37 g/g yield from glucose.
- *E. coli* Δ*edd*-pBSK-$CAB_{A\text{-}04}$ utilized crude glycerol to produce 74.8 wt% PHB in 24 h.
- The PHB yield reached 0.37 g/g from glucose and 0.20 g/g from crude glycerol.
- Δ*edd* in *E. coli* redirected carbon flux and enhanced PHB biosynthetic efficiency.

GRAPHICAL ABSTRACT

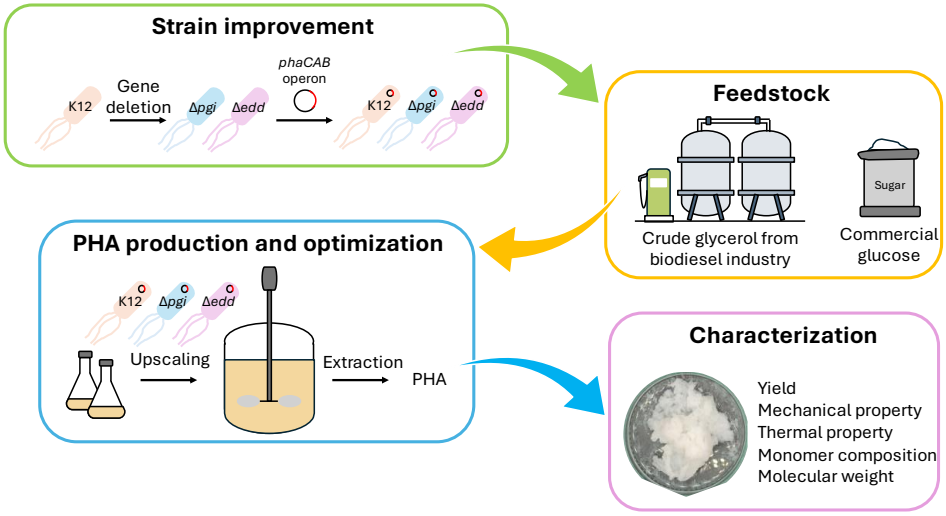

ARTICLE INFO

Article history:
Received 23 March 2025
Received in revised form 6 June 2025
Accepted 12 July 2025
Published 1 September 2025

Keywords:
Polyhydroxybutyrate
Pentose phosphate pathway
Escherichia coli
Life cycle impact
Green production

ABSTRACT

The biomaterial polyhydroxybutyrate (PHB) is a promising, renewable, and green alternative polymer. In this study, a method to incorporate gluconate 6-phosphate dehydratase (*edd*) deletion in *Escherichia coli* expressing PHB biosynthesis genes from *Cupriavidus necator* strain A-04 was proposed. The growth of the *edd*-deficient strain, which is defective in the glycolytic Entner–Doudoroff pathway, decreased significantly in Luria-Bertani (LB) medium supplemented with glucose. Surprisingly, compared with the wild-type strain, the recombinant *edd*-deficient strain expressing PHB biosynthesis genes exhibited expeditious PHB accumulation with a high PHB content. The *edd*-deficient strain reached the highest PHB concentration of 7.6 g/L and a 93 wt% PHB content within 30 h of flask-scale cultivation when commercial glucose was used as the sole carbon source. In addition, the resulting strain was able to utilize crude glycerol waste from the biodiesel industry for PHB accretion with a 74.8 wt% content in 24 h. The PHB yields obtained from glucose and crude glycerol waste were 0.37 and 0.20 g PHB/g substrate, respectively. These findings not only broaden the understanding of the effect of glucose metabolism on PHB production but also provide promising candidates for the production of polyhydroxyalkanoates in the future.

* Corresponding author at:
E-mail address: suchada.cha@chula.ac.th

Please cite this article as: Pachimsawat J., Tsuge T., Napathorn S.C. Rewiring *Escherichia coli* central carbon metabolism for the sustainable bioconversion of waste glycerol into biodegradable polyhydroxybutyrate. Biofuel Research Journal 47 (2025) 2451-2469. DOI: 10.18331/BRJ2025.12.3.2.

Contents

Abbreviation/Nomenclature

6PGL	6-phosphogluconolactonase	pBSK	pBluescript II SK (+)
6PGDH	6-phosphogluconate dehydrogenase	PDI	Polydispersity index
ALS	Aldolase	PEG	Polyethelene glycol
Amp	Ampicillin	PGI	Phosphoglucose isomerase
CDM	Cell dry mass	PGK	Phosphoglycerokinase
CsrA	Carbon storage regulator A	PGM	Phosphoglycerate mutase
DSC	Differential scanning calorimetry	PhaA	Beta-ketothiolase
E4P	D-erythrose-4-phosphate	PhaB	NADPH-dependent acetoacetyl-CoA reductase
EDA	Entner-Doudoroff aldolase	PhaC	PHA synthase
EDD	Gluconate 6-phosphate dehydratase	PhaP	Surface-binding protein of PHA granule
EDP	Entner-Doudoroff pathway	PHA	Polyhydroxyalkanoate
EMP	Embden-Meyerhof-Parnas pathway	PHB	polyhydroxybutyrate
ENO	Enolase	PKF	Phosphofructokinase
G6PDH	Glucose-6-phosphate dehydrogenase	pntAB	Membrane-bounded pyridine nucleotide transhydrogenase
GAPDH	Glyceraldehyde-3-phosphate dehydrogenase	PPP	Pentose phosphate pathway
GC	Gas chromatography	PYK	Pyruvate kinase
GPC	Gel permeation chromatography	RCM	Residual cell mass
HK	Hexokinase	RPE	Ribulose-5-phosphate epimerase
ΔH_m	Enthalpy of melting	RPI	Ribulose-5-phosphate isomerase
ΔH_f	Heat of fusion	TAL	Transaldolase
HPLC	High-performance liquid chromatography	TEM	Transmission electron microscopy
LB	Luria-Bertani	TKT	Transketolase
METAFoR	Metabolic flux ratio	T_c	Crystallization temperature
M_w	Weight average molecular weight	T_g	Glass transition temperature
M_n	Number average molecular weight	T_m	Melting temperature
NADPH	Reduced nicotinamide adenine dinucleotide phosphate	UdhA	Soluble transhydrogenase
OD	Optical density	%Xc	Percent crystallinity
P[3HB-*co*-4HB]	Poly(3-hydroxybutyrate-co-4-hydroxybutyrate)	$\gamma_{x/s}$	Yield of biomass per substrate
P[3HB-*co*-3HV]	Poly(3-hydroxybutyrate-co-3-hydroxyvalerate)	$\gamma_{p/s}$	Yield of product per substrate
P3HV	Poly(3-hydroxyvalerate)		

Please cite this article as: Pachimsawat J., Tsuge T., Napathorn S.C. Rewiring *Escherichia coli* central carbon metabolism for the sustainable bioconversion of waste glycerol into biodegradable polyhydroxybutyrate. Biofuel Research Journal 47 (2025) 2451-2469. DOI: 10.18331/BRJ2025.12.3.2.

1. Introduction

Polyhydroxybutyrate (PHB), a member of the polyhydroxyalkanoates (PHA) family, is a biobased polymer known for its biodegradability and biocompatibility. In natural systems, PHB is synthesized *via* a series of enzymatic reactions and accumulated intracellularly as cytoplasmic inclusion bodies, serving as carbon and energy storage in various microorganisms. In previous studies, the soil-isolated *Cupriavidus necator* strain A-04 with 99.78% 16S RNA sequence identity to the commercial strain *C. necator* strain H16 exhibited the ability to accumulate 78 wt% PHB from fructose, 20 wt% P(3-hydroxybutyrate-*co*-79%3-hydroxyvalerate) [P(3HB-*co*-79%3HV)] from valeric acid, 47 wt% P(3-hydroxybutyrate-*co*-20%4-hydroxybutyrate) [P(3HB-*co*-20%4HB)] from γ-hydroxybutyric acid lactone and terpolymer of P(4%3-hydroxybutyrate-*co*-3%3-hydroxyvalerate-*co*-93%4-hydroxybutyrate) [P(4%3HB-*co*-3%3HV-*co*-93%4HB)] from fructose, valeric acid and γ-hydroxybutyric acid as carbon sources, respectively (Chanprateep and Kulpreecha, 2006; Chanprateep et al., 2008).

A sequence analysis revealed that the PHA biosynthesis operon of *C. necator* strain A-04 was composed of three genes encoding β-ketothiolase (PhaA, 40.6 kDa, accession no. FJ897461), acetoacetyl-CoA reductase (PhaB, 26.4 kDa, accession no. FJ897462), and PHA synthase (PhaC, 64.3 kDa, accession no. FJ897463) (Napathorn et al., 2021). The biosynthesis of PHAs starts with the condensation of two molecules of acetyl-CoA by β-ketothiolase to form acetoacetyl-CoA. The acetoacetyl-CoA molecule is then reduced to 3-hydroxybutyryl-CoA with the aid of acetoacetyl-CoA reductase coupled to NADPH consumption. Finally, 3-hydroxybutyryl-CoA is polymerized by PHA synthase and forms PHA granules. Acetoacetyl-CoA reductase is generally known as an NADPH-preferring enzyme (Olavarria et al., 2022), although this enzyme has been reported to have activity toward NADH as well in other microorganisms (Ritchie et al., 1971).

Currently, the industrialization of PHA struggles with various challenges, including a high production cost and unstable PHA properties. Although natural PHA producers can synthesize PHA easily from various monomers, the efficiency of the process is limited only to the laboratory scale and from structurally related precursors (Favaro et al., 2019). Unlike natural PHA producers, *Escherichia coli* does not possess endogenous PHA depolymerases, causing intracellular polymer degradation and resulting in a low PHA content (Gebauer and Jendrossek, 2006). As a result, up to 90 wt% of the cellular dry weight of PHB could be accumulated by the genetic engineering of PHA synthase genes. Several strain improvement approaches were successfully achieved to increase PHA productivity. The deletion of carbon storage regulator A (*CsrA*) (Wu et al., 2020) and inactivation of cell fission genes (*minC* and *minD*) (Wu et al., 2016) resulted in a new division pattern and high cell density. Overexpression of *phaP* encoding the surface-binding protein of PHA granules led to smaller and densely packed PHA granules, resulting in a higher PHA content (Lee et al., 2023).

Reduced nicotinamide adenine dinucleotide phosphate (NADPH) serves as a key reducing equivalent required by essential enzymes involved in central biosynthetic pathways. Numerous studies have shown that NADPH availability represents a primary bottleneck in the biosynthesis of various intracellular products, including PHA. Cofactor engineering, which specifically targets the manipulation of intracellular NADPH levels, has been extensively investigated as a strategy to enhance PHA production efficiency (Lim et al., 2002; Lin et al., 2015; Ng et al., 2015). The overexpression of transhydrogenase enzymes, such as the membrane-bound pyridine nucleotide transhydrogenase (PntAB) and the soluble transhydrogenase (UdhA), has been shown to increase intracellular NADPH concentrations (Sauer et al., 2004; Sanchez et al., 2006). While cofactor engineering focuses on regulating specific metabolic nodes, metabolic engineering encompasses broader modifications across metabolic networks. Lin et al. (2015) introduced a threonine bypass strategy to increase the levels of acetyl-CoA and its derivatives, including PHA, resulting in a 3.3-fold increase in PHB production compared to the parental strain. Activation of the threonine bypass not only influences the PHA biosynthesis pathway but also affects related metabolic routes involving acetyl-CoA derivatives, glycine, threonine, and serine (Lin et al., 2015).

In the context of PHA biosynthesis, PHAs are synthesized from metabolic precursors derived from sugars *via* central carbon metabolism or from fatty acids through either β-oxidation or *de novo* synthesis. Glucose metabolism in *E. coli* involves three major pathways, the Embden–Meyerhof–Parnas pathway (EMP), the Entner–Doudoroff pathway (EDP), and the pentose phosphate pathway (PPP), each of which contributes to the regulation of PHA biosynthesis (**Fig. 1**). The genetic modification of glucose metabolism, such as deletion of the pgi gene encoding phosphoglucose isomerase, an essential enzyme in the EMP, has been explored to increase PHA accumulation. Protein expression analyses following *pgi* disruption revealed altered gene expression patterns due to redirected glucose flux, and bacterial growth was shown to increase in conjunction with PHA biosynthesis (Kabir and Shimizu, 2003a; Stincone et al., 2015; Xiong et al., 2025). However, consistent evidence indicating that *pgi* disruption results in significantly higher PHA accumulation compared to the parental strain is still lacking.

In contrast, our preliminary experiments demonstrated a negative impact of *pgi* disruption on PHA production. This finding prompted us to explore alternative strategies for engineering PHA biosynthesis by redirecting glucose metabolism through the EMP and the PPP. Gluconate 6-phosphate dehydratase (*edd)* and Entner–Doudoroff aldolase (*eda*) were investigated for effective targeted disruption and inactivation of the EDP pathway. The *edd* gene, which encodes the enzyme responsible for converting 6-phosphogluconate to 2-keto-3-deoxy-6-phosphogluconate (KDPG), is located at the key position at the initial branch point between the EDP and PPP pathways. In contrast, the *eda* gene functions at a subsequent step, catalyzing the cleavage of KDPG into pyruvate and glyceraldehyde-3-phosphate. Previous studies have shown that the deletion of *eda* leads to the intracellular accumulation of KDPG, which inhibits bacterial growth (Fuhrman et al., 1998). Therefore, targeting the *edd* gene may provide a more effective strategy for disrupting the EDP pathway, as illustrated in **Figure 1**.

Although the metabolic and biochemical consequences of *edd* gene deletion in *E. coli* have not been comprehensively characterized, existing studies have shown that *edd* disruption can increase the production of NADPH-dependent and PPP-related metabolites. For example, in *pgi* and *edd* double knockout strains, shikimic acid production was increased due to the increased availability of the PPP intermediate D-erythrose-4-phosphate (E4P) (Ahn et al., 2011). Similarly, *edd* deletion has been shown to promote inosine accumulation through increased synthesis of ribose-5-phosphate (Shimaoka et al., 2005) and to increase riboflavin production as a result of increased ribulose-5-phosphate levels (Lin et al., 2014). These findings collectively indicate that *edd* gene disruption redirects carbon flux into the PPP, the principal source of intracellular NADPH. Given that PHA biosynthesis is an NADPH-consuming process, the introduction of the PHA pathway into an *edd*-deficient background represents a promising strategy for increasing PHA production.

In this study, we investigated the effect of *edd* gene deletion on PHB production in *E. coli* strains engineered to express PHB biosynthesis genes from the *C. necator* strain A-04 (Chanprateep et al., 2008; Boontip et al., 2021; Napathorn et al., 2021). The resulting recombinant *E. coli* was cultivated using either commercial glucose or crude glycerol as the sole carbon source. Additionally, we characterized the fermentation parameters associated with PHB production in the *edd*-deficient strain. The outcomes of this work provide valuable insights into further metabolic engineering efforts aimed at improving the biosynthesis of PHAs and related bioproducts in recombinant *E. coli*.

2. Materials and Methods

2.1. Bacterial strains, plasmids, and culture conditions

The *E. coli* strains and plasmids used in this study are summarized in **Table 1**. *C. necator* strain A-04 served as the source for the $phaCAB_{A\text{-}04}$ operon. The *E. coli* strain JM109 was employed as the host for plasmid construction. *E. coli* K12, a parental strain, was used as the host for PHB production. *E. coli* strains deficient in *edd* and *pgi,* both derived from the *E. coli K-12* background, were obtained from the Keio collection (Baba et al., 2006). Stock cultures were prepared in a 15% (v/v) glycerol solution and stored at −80 °C. For routine cultivation, *E. coli* strains were grown in Luria–Bertani (LB) media containing 10 g/L tryptone (HiMedia Laboratories Pvt. Ltd., Mumbai, India), 5 g/L yeast extract (HiMedia Laboratories Pvt. Ltd., Mumbai, India), and 10 g/L NaCl (Merck KGaA, Darmstadt, Germany). Where necessary, antibiotics were added to the

Please cite this article as: Pachimsawat J., Tsuge T., Napathorn S.C. Rewiring *Escherichia coli* central carbon metabolism for the sustainable bioconversion of waste glycerol into biodegradable polyhydroxybutyrate. Biofuel Research Journal 47 (2025) 2451-2469. DOI: 10.18331/BRJ2025.12.3.2.

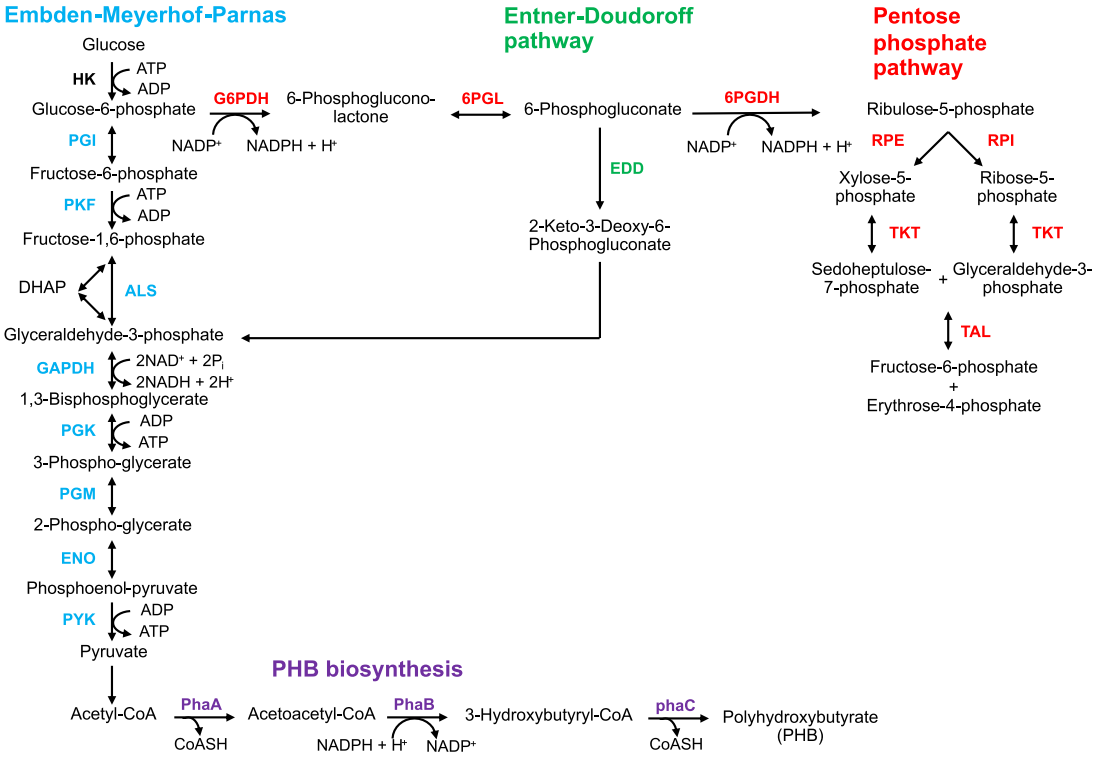

Fig. 1. Schematic diagram of central glucose metabolism, Embden–Meyerhof–Parnas, Entner–Doudoroff, pentose phosphate pathways, and poly(3-hydroxybutyrate) biosynthesis.

Table 1.
Strains and plasmids used in this study.

Name	Description	Ref.
Strains		
Cupriavidus necator A-04	Wild-type	Chanprateep et al. (2008)
E. coli K12	F-, Δ*(araD-araB)567,* Δ*lacZ4787*(::rrnB-3), λ-, *rph-1*, Δ*(rhaD-rhaB)568, hsdR514*	Promega Corporation, USA
E. coli Δ*pgi*	F-, Δ*(araD-araB)567,* Δ*lacZ4787*(::rrnB-3), λ-, *rph-1*, Δ*(rhaD-rhaB)568,* Δ*pgi-721::kan, hsdR514*	Baba et al. (2006)
E. coli Δ*edd*	F-, Δ*(araD-araB)567,* Δ*lacZ4787*(::rrnB-3), λ-, *rph-1*, Δ*(rhaD-rhaB)568,* Δ*edd-776::kan, hsdR514*	Baba et al. (2006)
E. coli JM109	F′*traD36 proA+B+ lacI*^{q}*(lacZ)ΔM15/Δ(lac-proAB) glnV44 e14- gyrA96 recA1 relA1 endA1 thi hsdR17*	Promega Corporation, USA
Plasmids		
pBluescript II SK (+)	A high copy number plasmid, Amp^{R}	Promega Corporation, USA
pBSK-*CAB*	A pBluescript II SK + derivative containing *phaCAB* operon from *Cupriavidus necator* A-04 with native promoter, Amp^{R}	**This Study**

medium at final concentrations of 100 μg/mL ampicillin or 50 μg/mL kanamycin (Sigma–Aldrich Corp., St. Louis, MO, USA). The cultures were incubated at 37 °C with shaking at 200 rpm for 16–18 h.

2.2. Construction of plasmids and recombinant strains

Standard molecular cloning procedures were employed for plasmid construction. The PCR products were purchased from Apsalagen Co., Ltd. (Apsalagen Co., Ltd., Bangkok, Thailand). DNA purification and plasmid isolation were performed using Favorgen plasmid DNA extraction kits (Favorgen Biotech Corp., Vienna, Austria). The oligonucleotide primers were synthesized by U2Bio Co., Ltd. (U2Bio Co., Ltd., Bangkok, Thailand). The plasmid pBSK-$CAB_{A\text{-}04}$ was constructed by amplifying the $phaCAB_{A\text{-}04}$ operon, including its native promoter, from *C. necator* strain A-04. Amplification was performed using the following primers: forward primer 5′-CATGGATCCTCACTCGTCCTTGCC-3′ and reverse primer 5′-CATGGATCCTATGCCCAACAAGGC-3′, with the *BamHI* restriction sites underlined. The resulting PCR product was purified and ligated into the pBluescript SK(+) vector at the *BamHI* site to generate pBSK-$CAB_{A\text{-}04}$. The integrity of the constructed plasmid was confirmed through the

Please cite this article as: Pachimsawat J., Tsuge T., Napathorn S.C. Rewiring *Escherichia coli* central carbon metabolism for the sustainable bioconversion of waste glycerol into biodegradable polyhydroxybutyrate. Biofuel Research Journal 47 (2025) 2451-2469. DOI: 10.18331/BRJ2025.12.3.2.

corresponding restriction enzyme analysis and DNA sequencing. Subsequently, the constructed vector pBSK-$CAB_{A\text{-}04}$ was transformed into *E. coli* K12, as well as into *edd*- and *pgi*-deficient derivatives of the K-12 strain. Finally, the resulting recombinant strains, *E. coli* K12-pBSK-$CAB_{A\text{-}04}$, Δ*edd*-pBSK-$CAB_{A\text{-}04}$, and Δ*pgi*-pBSK-$CAB_{A\text{-}04}$, were used in subsequent experiments.

2.3. Bacterial growth profile

Growth curves of *E. coli edd*- and *pgi*-deficient strains, along with K12, were generated to determine the growth profiles of the bacteria. First, all *E. coli* strains were cultivated on LB media for 16–18 h at 37 °C. A single colony of each strain was then inoculated into fresh LB media supplemented with various concentrations of glucose (0, 2.5, 5, 10, 15, or 20 g/L). Bacteria were subsequently cultivated at 37 °C and 200 rpm for 24 h. Cell suspensions from each condition were collected at 2-h intervals, and the turbidity was subsequently measured at 600 nm *via* a spectrophotometer. Kinetic parameters, including the generation time (h) and specific growth rate (1/h), were calculated accordingly. The generation time is the time required to double the initial bacterial population during the log phase and is calculated by the multiplicative inverse of the specific growth rate. The specific growth rate is defined as the rate of increase in the biomass of a cell population per unit of biomass concentration and is calculated with **Equation 1**:

$$\mu = \frac{\ln OD_2 - \ln OD_1}{t_2 - t_2} \quad \text{Eq. 1}$$

where OD_1 is the $OD_{600\ nm}$ at the initial time, OD_2 is the $OD_{600\ nm}$ at the final time, t_1 is the time at the initial state, and t_2 is the time at the final state.

2.4. Expression of pBSK-$CAB_{A\text{-}04}$ in E. coli K12, edd- and pgi-deficient strains

PHB production by the *E. coli* K12-pBSK-$CAB_{A\text{-}04}$, Δ*edd*-pBSK-$CAB_{A\text{-}04}$, and Δ*pgi*-pBSK-$CAB_{A\text{-}04}$ strains was studied. Shaker flask experiments were performed in 250-mL Erlenmeyer flasks containing 50 mL of LB medium supplemented with 100 μg/mL ampicillin. *E. coli* K12-pBSK-$CAB_{A\text{-}04}$, Δ*edd*-pBSK-$CAB_{A\text{-}04}$, and Δ*pgi*-pBSK-$CAB_{A\text{-}04}$ were first cultivated on LB plates, subsequently transferred to LB media, and cultured on a rotary incubator shaker (Innova 4300, New Brunswick Scientific Co., Inc., Edison, NJ, USA) at 200 rpm and 37 °C for 24 h. The seed cultures were inoculated into fresh LB media supplemented with 100 μg/mL ampicillin and 20 g/L glucose and cultivated at 37 °C for 48 h. Different parameters that affect PHB production efficiency, including the cultivation temperature, inoculum size, and glucose concentration, were investigated. The cultivation temperatures used in this experiment were 30 and 37 °C. Various amounts of preculture inoculum (1, 3, 5, and 10% v/v) and different concentrations of glucose (10, 20, 30, and 40 g/L) were examined. The number of colony-forming units was calculated using **Equation 2** (Bhuyan et al., 2023):

$$\text{CFU} = \frac{\text{No. of colonies} \times \text{Dilution factor}}{\text{Volume of culture plated}} \quad \text{Eq. 2}$$

The culture samples were collected at 6-h intervals, followed by centrifugation at 8,000 rpm for 20 min and drying at 60 °C for 2 d for further analysis. Crude glycerol obtained from BBGI Biodiesel Company Limited (BBGI-BI) was employed as the sole carbon source to minimize the cost of PHB production. The *E. coli* K12-pBSK-$CAB_{A\text{-}04}$, Δ*edd*-pBSK-$CAB_{A\text{-}04}$, and Δ*pgi*-pBSK-$CAB_{A\text{-}04}$ strains were cultivated in LB media supplemented with 20 g/L crude glycerol and 5% (v/v) inoculum at 30 °C for 48 h.

2.5. PHB production in a 5-L fermenter

Batch cultivation of PHB produced by *E. coli* Δ*edd*-pBSK-$CAB_{A\text{-}04}$ was scaled up in a 5-L bioreactor (MDL500, B.E. Marubishi Co., Ltd., Tokyo, Japan). A preculture was prepared in a 500-mL Erlenmeyer flask containing 100 mL of LB medium and cultivated on a rotary shaker at 37 °C and 200 rpm for 24 h. The preculture was then transferred into a 5-L bioreactor containing 2.7 L of LB medium supplemented with 100 mg/mL ampicillin, 20 g/L glucose, and 5% (v/v) inoculum at 30 °C. The agitation speed and air flow rate were 200 rpm and 1 mL/min, respectively. The samples were collected at 6-h intervals for 48 h.

2.6. Analytical methods

The intracellular PHB content was analyzed after 48 h of bacterial cultivation. Briefly, the bacteria in the culture broth were harvested by centrifugation (5804 R, Eppendorf SE, Hamburg, Germany) at 4000 rpm for 15 min, and the pellet was repeatedly washed with distilled water. Cell growth was assessed based on the cellular dry mass (CDM), which was determined by filtering 2 mL of the culture broth through preweighed cellulose nitrate membrane filters (pore size 0.22 μm; Sartorius AG, Göttingen, Germany). The filters were dried at 80 °C for 2 d and stored in desiccators before weighing. The residual biomass (RCM), which represents the net bacterial biomass, was calculated by subtracting the PHB content from the CDM. The dried cells were then subjected to methanolysis for PHB quantification. The PHB concentration was determined using a methyl esterification method involving a mixture of chloroform and 15% (v/v) methanol–sulfuric acid (1:1, v/v). The mixture was incubated at 80 °C for 3 h. After cooling to room temperature, distilled water was added to induce phase separation. The organic phase containing the PHAs was filtered and transferred to a gas chromatography (GC) vial for analysis. Monomeric methyl esters produced from methanolysis were quantified using a gas chromatograph (CP3800, Varian Inc., Walnut Creek, CA, USA) equipped with a Carbowax-PEG capillary column (60 m length, 0.25 mm ID, 0.25 μm film thickness; Varian Inc., Walnut Creek, CA, USA). Benzoic acid and commercially available PHB (Sigma–Aldrich Corp., St. Louis, MO, USA) were used as the internal and external standards, respectively (Phothong et al., 2024a).

For the copolymer composition analysis (mol%) of 3HB and 3HV, 8 mol% P(3HB-*co*-3HV) (Sigma–Aldrich Corp., St. Louis, MO, United States) was used as an external standard. PHB productivity (g/L·h) was calculated, and the PHB yield (g/g) was defined as the amount of PHB (g) produced per gram of glucose consumed. The culture supernatants were filtered through a 0.22-μm nylon syringe filter to determine the glucose, glycerol, and ethanol concentrations. The filtrates were analyzed with a high-performance liquid chromatography (HPLC) system (Agilent 1200 Infinity Series, Agilent Technologies Inc., Santa Clara, CA, USA) equipped with a 1260 refractive index detector (RID) and X-bridge-BEH amide column (4.6 × 250 mm, 5 μm; Waters Corp, Milford, MA, USA). The isocratic mobile phase was acetonitrile/water mixtures of 60:40 (v/v) for glucose and 70:30 (v/v) for glycerol at a flow rate of 1.0 mL/min and a temperature of 30°C. A reverse-phase Nova-Pak C18 column (3.9 × 150 mm) (Waters Corp, Milford, MA, USA) with a mobile phase of 70:30 acetonitrile/water was used to analyze the ethanol concentration. A flow rate of 1.0 mL/min and a temperature of 30°C were set for all the conditions (Simonzadeh and Ronsen, 2012).

2.7. PHB extraction, purification, and preparation of the PHB film

PHB that accumulated in bacterial cells was extracted using hot chloroform in a Soxhlet extractor, followed by three rounds of precipitation with *n*-hexane to increase the purity. The purified PHB polymers were dried via solvent evaporation and stored at room temperature. PHB films were prepared for mechanical property tests following ASTM standard D882-91 using a conventional solvent-casting technique. Specifically, PHB powder was dissolved in chloroform at a concentration of 1% (w/v), with 5 mL of chloroform used to control the film thickness. The resulting solution was poured onto a glass tray (Pyrex, Corning Inc., Corning, NY, USA) serving as the casting surface, followed by complete solvent evaporation under ambient conditions. The resulting films were then cut into strips measuring 50 × 150 mm, with at least ten samples prepared. Before analysis, the films were aged for four weeks to achieve equilibrium crystallization (Wongmoon and Napathorn, 2022; Phothong et al., 2024a).

2.8. Polymer molecular weight analysis

The weight-average molecular weight (M_w), number-average molecular weight (M_n), and polydispersity index (PDI) of the polymer were

Please cite this article as: Pachimsawat J., Tsuge T., Napathorn S.C. Rewiring *Escherichia coli* central carbon metabolism for the sustainable bioconversion of waste glycerol into biodegradable polyhydroxybutyrate. Biofuel Research Journal 47 (2025) 2451-2469. DOI: 10.18331/BRJ2025.12.3.2.

determined using gel permeation chromatography (GPC) on a Shimadzu LC20AD and CTO-20A system (Shimadzu Co., Ltd., Kyoto, Japan), equipped with a Shimadzu RID-10A refractive index detector and four Shodex columns (GPC K-802.5, 803, 804, and 805) connected in series (Resonac Co., Ltd., Tokyo, Japan). The PHB polymer was first dissolved in 0.1% (w/v) chloroform and filtered through a 0.45-µm Durapore® (PVDF) membrane filter with a low protein-binding capacity (Millex® -HV, Merck Millipore Ltd., Cork, Ireland). Styrene standards were used to prepare standard curves. The analysis was conducted at 40 °C using chloroform as the eluent, with a flow rate of 1 mL/min and an injection volume of 20 µL. M_w represents the weight-average molecular weight, which reflects the average molecular weight of all molecules in the sample weighted by their mass. M_n represents the number-average molecular weight, which was calculated based on the number of molecules at each molecular weight. The PDI, an indicator of the molecular weight distribution, was calculated as the ratio of M_w to M_n (PDI = M_w/M_n).

2.9. Thermal analysis by differential scanning calorimetry

The thermal properties of the PHB polymer were analyzed using differential scanning calorimetry (DSC) on a DSC7 instrument (PerkinElmer, Inc., Waltham, MA, USA) at the Petroleum and Petrochemical College, Chulalongkorn University. The measurements were conducted under a nitrogen atmosphere to prevent oxidative degradation. A PHB sample (10–20 mg) was sealed in an aluminum sample pan and placed in the DSC apparatus. The system was operated using STARe software (version SW 10.00; Mettler-Toledo International Inc., Columbus, OH, USA). The sample was initially heated from ambient temperature to 230 °C at a heating rate of 20 °C/min, held isothermally at 230 °C for 5 min, then cooled to −50 °C at the same rate. Subsequently, the sample was reheated to 230 °C at 20 °C/min, also under a nitrogen atmosphere. DSC thermograms were recorded to determine the thermal parameters. The melting temperature (T_m) was identified as the intersection point between the extrapolated baseline and the tangent at the peak of the endothermic transition. The enthalpy of melting (ΔH_m) was calculated as the area under the melting peak relative to the baseline. The glass transition temperature (T_g) was determined by extrapolating the midpoint of the step change in heat capacity observed between the glassy and rubbery states upon heating the quenched sample. The degree of crystallinity (XC-DSC) of PHB was calculated using **Equation 3** (Seoane et al., 2018):

$$X_{C-DSC}(\%) = \frac{\Delta H_m}{\Delta H_m^0} \times 100 \quad \text{Eq. 3}$$

where ΔH_m is the measured melting enthalpy of the sample, and ΔH^0_m is the theoretical melting enthalpy of 100% crystalline PHB, which was set as 146 J/g (Barham et al., 1984).

The mechanical properties of PHB, such as elongation (%), stress (MPa), toughness (MPa), and Young's modulus, were analyzed using a universal testing machine (Lloyd LRX, Lloyd Instruments Ltd., Bognor Regis, UK) with a crosshead speed of 10 mm/min.

2.10. PHB granule observation by transmission electron microscopy

Cell morphology and PHA granules were observed using a transmission electron microscope (TEM) at the Scientific and Technological Research Equipment Center, Chulalongkorn University, Bangkok, Thailand. The cell cultures were collected at the end of the 48-h fermentation period, cooled on ice, and harvested by centrifugation at 4000 rpm. The cell pellets were resuspended in 2.5% (v/v) glutaraldehyde prepared in 0.1 M phosphate buffer (pH 7.4) for primary fixation. Postfixation was performed using the addition of 1% (v/v) osmium tetroxide in the same buffer. The samples were dehydrated through a graded ethanol series (35%, 70%, 95%, and 100% v/v), followed by infiltration with Spurr's resin (Electron Microscopy Sciences, PA, USA). Ultrathin sections were obtained using an LKB 2088 Ultratome V (Surrey, UK), stained with 2% (w/v) uranyl acetate and 2% (w/v) lead citrate, and examined with a JEM-2100 transmission electron microscope (JEOL Ltd., Tokyo, Japan) at an accelerating voltage of 80 kV. TEM images of the microbial populations were analyzed with ImageJ software (the National Institute of Mental Health, Bethesda, MD, USA). The images were first changed to a grayscale format. The scale was calibrated by pixel-to-length. The sizes of the PHB granules and whole-cell areas were analyzed, along with the number of PHB granules per cell.

2.11. Statistical analysis

Statistical significance was assessed using either an unpaired Student's t test for pairwise comparisons or one-way analysis of variance (ANOVA) followed by the Bonferroni correction for multiple comparisons. The data from three independent biological replicates are presented as the means ± standard deviations (SDs). Statistical analyses were performed using SPSS version 22 (IBM Corp., Armonk, NY, USA), and differences were considered statistically significant at $p \leq 0.05$.

3. Results and Discussion

3.1. Bacterial growth of E. coli mutants and parental strains

E. coli strain K12 represented the parental strain, whereas *edd*- and *pgi*-deficient strains presented inactivation of the EDP and EMP pathways, respectively (**Fig. 1**). All strains were cultivated at 37 °C for 24 h in LB medium supplemented with different concentrations of glucose, and the growth rate was determined by measuring the turbidity of the cell suspensions at 600 nm using a spectrophotometer. The forward scatter signal intensity is proportional to the concentration of bacterial cells in suspensions. The results of the bacterial growth evaluation of *E. coli edd*- and *pgi*-deficient strains, along with the K12 strain, are presented in **Table 2**. The parental *E. coli* K12 strain exhibited a similar pattern of growth in both the absence and presence of glucose in LB medium (**Supplementary Information, Fig. S1a**). The maximum OD_{600} of the *E. coli* strain K12 at each glucose concentration (0–20 g/L) ranged between 2.9±0.1 and 3.1±0.0. In the absence of glucose, the specific growth rate of the *E. coli* K12 strain was 0.25 1/h, with a doubling time of 0.07 h.

Compared with medium without glucose, the addition of glucose to the medium resulted in a slight decrease in the growth of the *E. coli* K12 strain (**Supplementary Information, Figs. S1b–f**). The specific growth rate of the *E. coli* K12 strain cultivated in media containing various concentrations of glucose ranged from 0.24 to 0.25 1/h, with a doubling time of 0.070 h. Interestingly, the decrease in the growth of the *E. coli* K12 strain did not directly change with the glucose concentration. Thus, the statistical analysis suggested that the addition of glucose had no significant effect on the growth of the *E. coli* K12 strain ($p > 0.05$). Zhang et al. (2005) reported that the addition of glucose to the medium increased the growth rate of *E. coli* in functional interaction studies between carbon and an iron regulatory system. Similar results were obtained by Suresh et al. (2023), who reported that the increase in *P. aeruginosa* growth varied proportionally to the amount of glucose supplied. This information indicated the importance of the media type on the growth of bacteria assimilating glucose as a carbon source. The main reason for this effect is likely that glucose could promote the extra growth of bacteria, particularly in nutrient-depleted media, which was used by Suresh et al. (2023) and Zhang et al. (2005). In addition, Vasiljevs et al. (2023) demonstrated the difference in the effect of glucose on bacterial growth in nutrient-rich and nutrient-limited media.

In the absence of glucose, the *E. coli edd*- and *pgi*-deficient strains had a similar pattern to that of the *E. coli* K12 strain and reached maximum OD_{600} values of 3.0±0.0 and 2.9±0.0, respectively. The specific growth rates of these strains were 0.24 and 0.23 1/h, with a doubling time of 0.07 h. However, the growth rates of the *E. coli edd*- and *pgi*-deficient strains decreased over time in the presence of glucose (2.5–20 g/L). The OD_{600} decreased drastically to approximately 1.7 for *E. coli* Δ*edd* and 1.9 for *E. coli* Δ*pgi* when glucose was added to the medium. The specific growth rate decreased to 0.20–0.22 1/h, whereas the doubling time inversely increased to 0.08 h in the mutant strains. The specific growth rate was 0.24–0.25 1/h, and the doubling time was 0.07 h in the wild-type strain *E. coli* K12. Despite the difference in glucose concentration, both the *E. coli edd*- and *pgi*-deficient strains were affected identically and attained similar growth values. The growth kinetic parameters suggested that metabolic perturbation enhanced the cell proliferation process and decreased cell growth in *E. coli edd*- and *pgi*-deficient strains when glucose was supplied as a carbon source. Unlike the *E. coli* K12 strain, the glucose concentration had a significant effect on the growth of the *E. coli edd*- and *pgi*-deficient strains ($p < 0.05$), which may be due to NADPH accumulation and cellular perturbations.

Please cite this article as: Pachimsawat J., Tsuge T., Napathorn S.C. Rewiring *Escherichia coli* central carbon metabolism for the sustainable bioconversion of waste glycerol into biodegradable polyhydroxybutyrate. Biofuel Research Journal 47 (2025) 2451-2469. DOI: 10.18331/BRJ2025.12.3.2.

Table 2.
Growth measurement and kinetics of *E. coli* strain K12, Δ*edd* and Δ*pgi* cultivated in LB medium supplemented with various glucose concentrations at 37 °C.

***E. coli* Strain**	**Maximum OD_{600}[1]**	**Specific Growth Rate (1/h)**	**Doubling Time (h)**
0 g/L glucose			
K12	3.1 ± 0.0[a2]	0.25	0.07
Δ*edd*	3.0 ± 0.0[a]	0.24	0.07
Δ*pgi*	2.9 ± 0.0[a]	0.23	0.07
2.5 g/L glucose			
K12	3.2 ± 0.0[a]	0.24	0.07
Δ*edd*	1.9 ± 0.0[b]	0.20	0.08
Δ*pgi*	1.9 ± 0.0[b]	0.21	0.08
5 g/L glucose			
K12	3.1 ± 0.0[a]	0.24	0.07
Δ*edd*	1.7 ± 0.0[b]	0.21	0.08
Δ*pgi*	1.9 ± 0.0[b]	0.22	0.08
10 g/L glucose			
K12	3.0 ± 0.0[a]	0.24	0.07
Δ*edd*	1.7 ± 0.0[b]	0.22	0.08
Δ*pgi*	1.9 ± 0.0[b]	0.22	0.08
15 g/L glucose			
K12	3.1 ± 0.1[a]	0.25	0.07
Δ*edd*	1.7 ± 0.0[b]	0.20	0.08
Δ*pgi*	1.9 ± 0.0[b]	0.22	0.08
20 g/L glucose			
K12	2.9 ± 0.1[a]	0.24	0.07
Δ*edd*	1.7 ± 0.0[b]	0.22	0.07
Δ*pgi*	2.0 ± 0.0[b]	0.22	0.08

[1] Results are expressed as mean ± SD (n = 3).
[2] The different superscript letters within the same column are significantly different at $p < 0.05$.

The distribution of carbon flux in the central metabolism of *E. coli* grown on glucose is illustrated in **Figure 2**. In wild-type *E. coli*, the majority of glucose-derived carbon is metabolized through the EMP pathway, which accounts for approximately 69–88% of the total carbon flux (Rui et al., 2010). The residual carbon flux is channeled through the PPP, which is highly dynamic and responsive to cellular demands and alternative carbon sources, whereas the EDP functions as an auxiliary route for glucose metabolism. Disruption of the *pgi* gene, a key component of the EMP pathway, has been shown to substantially impair bacterial growth and glucose consumption (Canonaco et al., 2001; Charusanti et al., 2010). An analysis of the metabolic flux ratio (METAFoR) has shown that in *pgi*-deficient strains, the PPP becomes the dominant pathway for glucose catabolism (Canonaco et al., 2001; Sauer et al., 2004). Similarly, the deletion of *edd*, a gene encoding 6-phosphogluconate dehydratase in the EDP, also led to the rerouting of carbon flux through the PPP, as evidenced by the increased production of PPP-derived compounds such as inosine and riboflavin (Shimaoka et al., 2005; Lin et al., 2014). Bennett et al. (2020) also reported that *edd* deletion results in a metabolic imbalance, notably the accumulation of ribulose-5-phosphate, a central PPP intermediate, as confirmed by a metabolic flux analysis (Bennett et al., 2020).

While previous strategies, such as *pgi* deletion or cofactor engineering (e.g., overexpression of transhydrogenases or enhancement of NADPH supply pathways), also redirect flux to the PPP, they often lead to excessive NADPH accumulation. This redox imbalance can severely impair cellular homeostasis, resulting in DNA damage, protein oxidation, lipid peroxidation, and ultimately growth inhibition or cell death (Siedler et al., 2012). In contrast, *edd* deletion represents a more subtle and potentially advantageous approach. By selectively impairing the EDP, it promotes PPP flux without entirely blocking glycolysis or disrupting key EMP enzymes. This modulation may allow for more balanced NADPH production, mitigating the adverse effects associated with NADPH overaccumulation while still enhancing the biosynthetic capacity of the cell.

3.2. PHB optimization and PHB accumulation in the E. coli K12, edd- and pgi-deficient strains harboring PHA biosynthetic genes from C. necator strain A-04

As a result of triggering the PPP, *edd*- and *pgi*-deficient strains accumulated large amounts of intracellular NADPH. Many researchers are

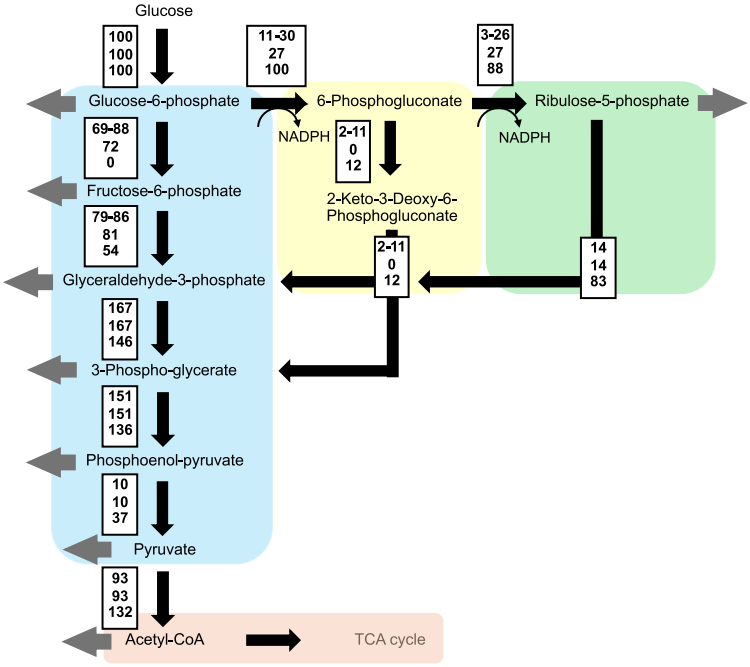

Fig. 2. Distribution of carbon flux in the central metabolism of the *E. coli* wild-type (top values), Δ*edd* (middle values), and Δ*pgi* (bottom values) strains during maximum exponential growth on glucose. The estimated net fluxes in the white rectangles are molar percentages of the mean specific glucose uptake rates. The inactivated reactions were omitted from the network that was used for data analysis. Arrowheads indicate the direction of a given flux (Sauer et al., 2004; Rui et al., 2010; Long and Antoniewicz, 2019; Bennett et al., 2020).

Please cite this article as: Pachimsawat J., Tsuge T., Napathorn S.C. Rewiring *Escherichia coli* central carbon metabolism for the sustainable bioconversion of waste glycerol into biodegradable polyhydroxybutyrate. Biofuel Research Journal 47 (2025) 2451-2469. DOI: 10.18331/BRJ2025.12.3.2.

aware of the importance of NADPH availability and aim to assess the maximum benefit of NADPH-producing bacteria. Similarly, the incorporation of the NADPH-consuming pathway, such as the PHA biosynthesis pathway, is ideal to recover cell growth and channel the use of NADPH to promote PHA production. The pBSK-CAB_{A-04} plasmid was introduced into the *E. coli* K12, *edd*- and *pgi*-deficient strains, and PHB production was studied. Several parameters, such as the cultivation temperature, inoculum concentration, and glucose concentration, affecting PHA production by recombinant *E. coli* were studied for optimization.

Two different temperatures (30 °C and 37 °C) were investigated to optimize PHA production in *E. coli* harboring pBSK-CAB_{A-04} (Fig. 3). In the presence of glucose, the cultivation of PHA-producing bacteria at 30 °C significantly increased overall growth and PHB production compared with that at 37 °C ($p < 0.05$). The results revealed that the highest CDM values of *E. coli* Δ*edd*-pBSK-CAB_{A-04}, Δ*pgi*-pBSK-CAB_{A-04} and K12-pBSK-CAB_{A-04} were observed at a cultivation temperature of 30 °C (4.0±0.2, 3.2±0.3 and 3.3 ± 0.3 g/L, respectively) in media supplemented with glucose, whereas a reduction in the CDM of all the strains of approximately 52% was observed at 37 °C. The main reason why PHA production was increased at 30°C could be the specific activity of PHA synthase, a key enzyme in PHA polymerization, from the mesophilic *C. necator* H16, which was maximized at 30 °C (Sheu et al., 2012). Nevertheless, the results revealed that all strains of *E. coli* harboring pBSK-CAB_{A-04} exhibited greater growth at 37 °C in the absence of glucose in the medium. Changing the cultivation temperature to 30 °C greatly affected bacterial growth, especially that of the *E. coli edd*- and *pgi*-deficient strains (0.8 and 0.5 g/L CDM, respectively), in media without glucose. These results suggest that different temperatures are needed for the preculture preparation and fermentation of PHB. Thus, precultures were prepared by cultivating the bacteria at 37 °C in the absence of glucose, and PHB production was induced by cultivating the precultures in freshly prepared media supplemented with glucose at 30 °C to obtain the optimized conditions.

Different amounts of inoculum (1, 3, 5 and 10% (v/v)) were inoculated into fresh LB medium supplemented with 20 g/L glucose and cultivated at 30 °C to study the effects of the inoculum concentration on PHB accumulation. The time course of bacterial growth and PHB accumulation is presented in Figure 4. Overall, a 3–5% (v/v) inoculum concentration resulted in similar results, in which the CDM reached 3.2–3.5 g/L with a 55.5–59.2 wt% PHB content in 24 h. The statistical analysis revealed that the inoculum size significantly differed from the CDM and PHB accumulation ($p < 0.05$). Fermentation kinetic parameters were calculated to distinguish each condition, and the best conditions for PHB production were evaluated (Table 3). The results showed that when a 5% inoculum with 6×10^6 CFUs/mL (data not shown) was used, the maximum PHB yield peaked at 0.20 g PHB/g glucose, with a volumetric productivity of 0.09 g/L·h. Therefore, an inoculum concentration of 5% (v/v) was used in subsequent experiments.

The effects of different concentrations of glucose (10, 20, 30, and 40 g/L) on PHB production were examined in *E. coli* strain K12 (Table 4). The results indicated that different glucose concentrations significantly affected both the CDM and PHB concentrations ($p < 0.05$). Using 10 g/L glucose, a maximum CDM of 2.9±0.0 g/L and a PHB content of 38.7 wt% were achieved within 24 h. The addition of glucose concentrations ranging from 10 to 30 g/L resulted in higher CDM and PHB concentrations, reflecting insufficient amounts of glucose for PHB production at 10 g/L glucose. The CDM and PHB contents peaked at 2.8 and 48.2–48.8 wt%, with biomass and product yields of 0.1 g RCM/g glucose and 0.11–0.12 g PHB/g glucose, respectively, in the presence of 20 and 30 g/L glucose in the medium. As expected, the CDM and PHB concentrations obtained with 40 g/L glucose were the lowest, with a PHB yield of only 0.08 g PHB/g glucose. Although 20 and 30 g/L glucose yielded similar results, approximately 18 g/L glucose remained in the medium at the end of fermentation after starting with 30 g/L glucose (data not shown). A glucose concentration of 20 g/L was selected for use in further experiments to consider a cost-effective system.

3.3. PHB accumulation in E. coli edd- and pgi-deficient strains and the K12 strain harboring pBSK-CAB_{A-04} under the optimum conditions

In previous experiments, we expressed *phaCAB* from the *C. necator* strain A-04 in recombinant *E. coli* to produce PHB. When *E. coli edd*- and *pgi*-deficient strains and the K12 strain were cultivated in LB media supplemented with glucose, no PHB accumulation was detected in *E. coli* (Supplementary Information, Fig. S1). Therefore, the accumulation of PHB in *E. coli* harboring pBSK-CAB_{A-04} confirmed the function of the *phaCAB* operon. The time courses of PHB production by *E. coli* Δ*edd*-pBSK-CAB_{A-04}, Δ*pgi*-pBSK-CAB_{A-04}, and K12-pBSK-CAB_{A-04} are shown in Figure 5. After 24 h of cultivation, Δ*edd*-pBSK-CAB_{A-04} strongly accumulated CDM at 7.5 g/L, with a PHB content of up to 91 wt%. Compared with that of the *E. coli* K12-pBSK-CAB_{A-04} strain, the PHB content of *E. coli* Δ*edd*-pBSK-CAB_{A-04} increased by 24%, resulting in a 35% increase in the PHB concentration. In contrast, *E. coli* Δ*pgi*-pBSK-CAB_{A-04} had a slower growth rate, with 5.1 g/L CDM and 60.3 wt% PHB content. *E. coli* Δ*pgi*-pBSK-CAB_{A-04} presented a PHB content that was approximately 18% lower than that of the parental strain K12. At 48 h of cultivation, the CDW values of *E. coli* Δ*edd*-pBSK-CAB_{A-04} and K12-pBSK-CAB_{A-04} were comparable, with values of 9.3±0.5 and 9.7±0.5 g/L, respectively (Table 5). Even though *E. coli* Δ*edd*-pBSK-CAB_{A-04} had a lower CDM; this strain could accumulate PHB at concentrations as high as 81 wt%, resulting in a 7.6 g/L PHB concentration. *E. coli* K12-pBSK-CAB_{A-04} stored concentrations of 76.5 wt% and 7.3 g/L PHB at 48 h. In contrast, *E. coli* Δ*pgi*-pBSK-CAB_{A-04} presented a 7.8 g/L CDM with a PHB content of 72.4 wt%, which was lower than that of both *E. coli* Δ*edd*-pBSK-CAB_{A-04} and K12-pBSK-CAB_{A-04}.

Fermentation kinetic parameters were calculated to analyze the effectiveness of PHB production (Table 5). The specific growth rates of *E. coli* Δ*edd*-pBSK-CAB_{A-04} and Δ*pgi*-pBSK-CAB_{A-04} were 0.05 and 0.06 1/h, respectively, whereas that of *E. coli* K12-pBSK-CAB_{A-04} was 0.05 1/h. Interestingly, *E. coli* Δ*edd*-pBSK-CAB_{A-04} had a specific production rate of 0.21 1/h, which was the highest value among all three strains of *E. coli* used in this study. The productivity of *E. coli* Δ*edd*-pBSK-CAB_{A-04} was similar to that of *E. coli* K12-pBSK-CAB_{A-04}, with values ranging from 0.24 to 0.25 g/L·h, whereas that of *E. coli* Δ*pgi*-pBSK-CAB_{A-04} was only 0.15 g/L·h. Notably, the PHB yield (g of PHB per g of glucose) in *E. coli* Δ*edd*-pBSK-CAB_{A-04} increased to 0.37 g/g, whereas the theoretical yield of PHB from glucose was 0.478 g/g (Sun et al., 2020).

The data revealed the effects of EDP and EMP pathway disruptions on PHB production in *E. coli,* in which the EDP pathway disruption tended to have a positive effect on PHB production, whereas the bacteria with an EMP pathway disruption were likely to produce less PHB than the parental strain. These data were consistent with the report from Kabir and Shimizu (2003a), which described the use of the EMP pathway-disrupted strain for PHB production**.** The gene expression pattern of the *E. coli pgi*-deficient strain determined by RT–PCR showed that genes involved in the PPP pathway were substantially affected by the overexpression of genes involved in the PHA biosynthesis pathway, whereas most genes involved in the TCA cycle were downregulated. The growth of the *E. coli pgi*-deficient strain was suppressed due to the overproduction of NADPH *via* the PPP. The incorporation of the PHB biosynthesis pathway could restore cell growth to some extent. Although researchers have assumed that the *E. coli pgi*-deficient strain increased PHB production (Kabir and Shimizu, 2003b; Kim et al., 2022), the results from this experiment did not confirm this hypothesis.

Interestingly, no reports of PHB production in *E. coli* with an EDP pathway disruption are available. Thus, we introduced an innovative tool to increase PHB production by carbon metabolism redirection through EDP disruption. Meyer et al. (2018) reported that the disruption of the EDP pathway resulted in the accumulation of ribulose 5-phosphate via the PPP pathway by 6-phosphogluconate dehydrogenase (*gnd*). Moreover, the idea of deleting *pgi* and *edd* to divert glucose carbon flux into the PPP, together with deleting *rpi*, which blocks the nonoxidative pathway of the PPP to ensure optimal carbon flow through the oxidative pathway of the PPP, was presented by Bennett et al. (2020). Unfortunately, *E. coli* Δ*pgi*Δ*edd*Δ*rpiAB* did not grow in media supplemented with glucose and methanol, even when strain construction was successful (Bennett et al., 2020). Based on this evidence, we hypothesized that the deletion of the *edd* gene could reroute carbon flux into two important pathways, the EMP and PPP, and promote PHB production. The results of this study emphasized the positive effect of EDP disruption on PHB production (Fig. 5).

One possible explanation for the increase in PHB production was that the blockade of the EDP provided larger amounts of common intermediates for other metabolic pathways. PHB biosynthesis is highly dependent on the

Please cite this article as: Pachimsawat J., Tsuge T., Napathorn S.C. Rewiring *Escherichia coli* central carbon metabolism for the sustainable bioconversion of waste glycerol into biodegradable polyhydroxybutyrate. Biofuel Research Journal 47 (2025) 2451-2469. DOI: 10.18331/BRJ2025.12.3.2.

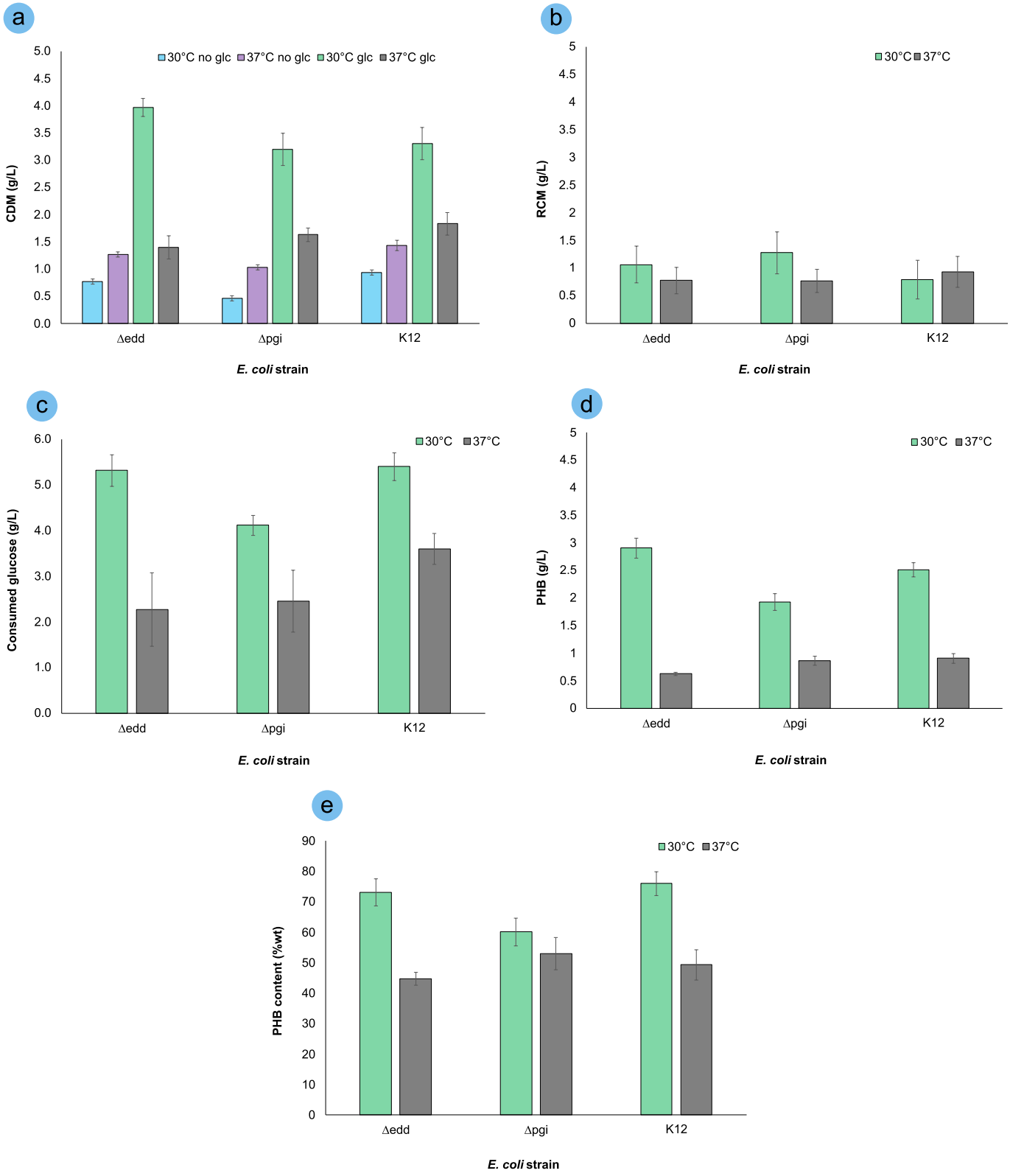

Fig. 3. Effects of temperature, 30 and 37 °C on **(a)** the biomass, **(b)** residual cell mass, **(c)** consumed glucose concentration, **(d)** PHB concentration, and **(e)** PHB content of *E. coli* Δ*edd*-pBSK-$CAB_{A\text{-}04}$, Δ*pgi*-pBSK-$CAB_{A\text{-}04}$, and *E. coli* K12-pBSK-$CAB_{A\text{-}04}$ using 1% inoculum concentration in LB medium supplemented with 20 g/L glucose and without glucose cultivated for 24 h.

Please cite this article as: Pachimsawat J., Tsuge T., Napathorn S.C. Rewiring *Escherichia coli* central carbon metabolism for the sustainable bioconversion of waste glycerol into biodegradable polyhydroxybutyrate. Biofuel Research Journal 47 (2025) 2451-2469. DOI: 10.18331/BRJ2025.12.3.2.

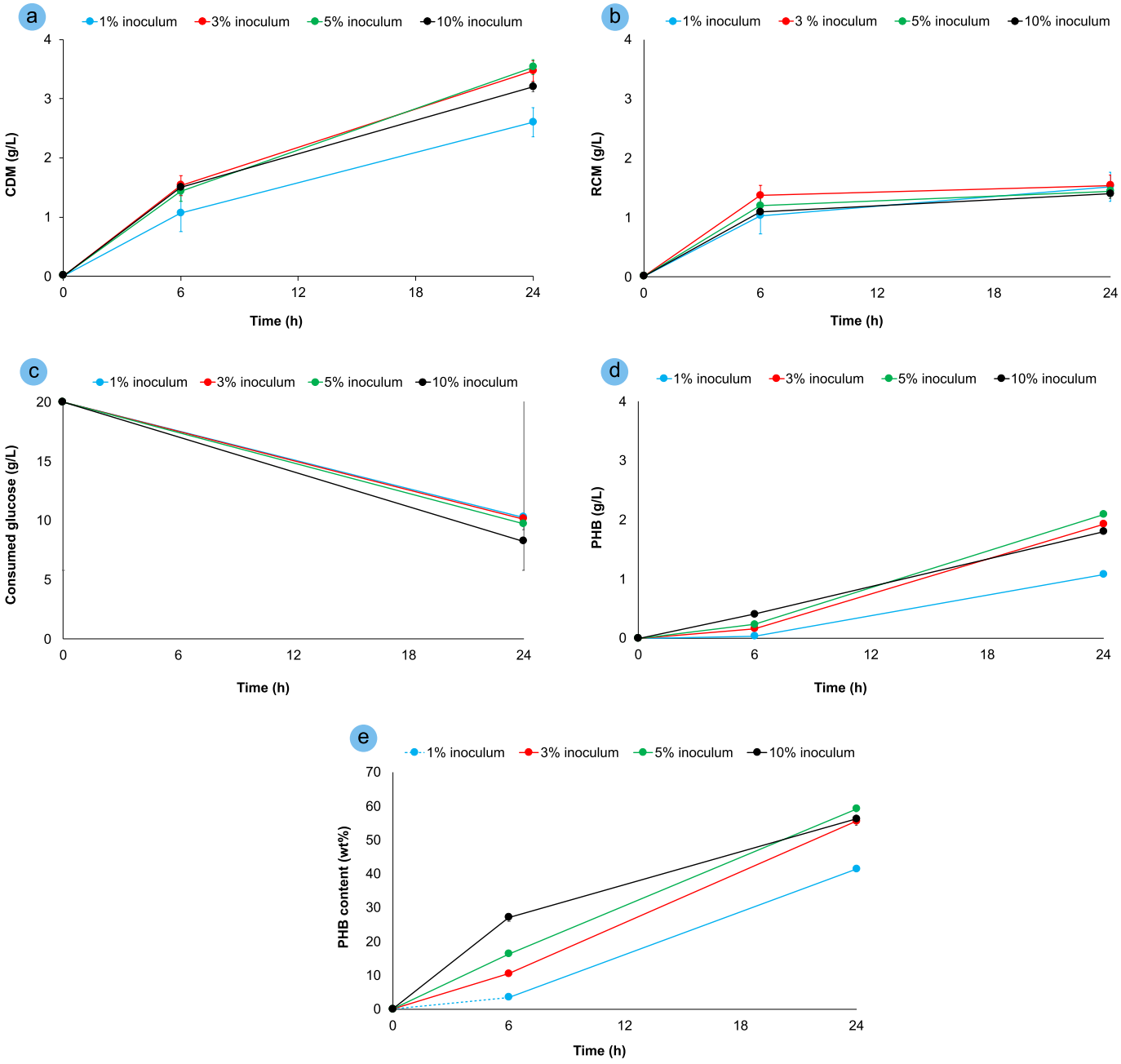

Fig. 4. Effects of the inoculum concentration on **(a)** the biomass, **(b)** residual cell mass, **(c)** consumed glucose concentration, **(d)** PHB concentration, and **(e)** PHB content of *E. coli* K12-pBSK-*CAB*$_{A\text{-}04}$ cultivated at 30 °C in LB medium supplemented with 20 g/L glucose for 24 h.

concentrations of acetyl-CoA, acetoacetyl-CoA, and 3-hydroxybutyryl-CoA, which are affected by the presence of the TCA cycle (Janasch et al., 2022). In addition, another possible reason for the increased PHB level was the increase in the intracellular NADPH level from the PPP. Since NADPH serves as a cofactor for acetoacetyl-CoA reductase, the availability of NADPH is crucial for PHB biosynthesis. EDP disruption redirected carbon flow through the EMP, the main source of acetyl-CoA, and the PPP, the main source of NADPH, to further promote PHB production.

Economic analyses of industrial PHA production indicate that over 40% of the total production cost is attributed to the feedstock. The reported production costs of PHA vary depending on the carbon source, with estimates of USD8.32/kg using sucrose (Lee and Choi, 1998), USD5.35–10.70/kg using glucose (Koller et al., 2007), USD5.38/kg using acetic acid (Mudliar et al., 2008), and USD3.63/kg using fructose (Akkoyunlu et al., 2024). As a result, increasing attention has been directed toward the use of low-cost byproducts and waste materials from agro-industrial processes as alternative, sustainable feedstocks for the production of value-added bioproducts. Recent studies have explored the use of various agrobased materials, including sugarcane derivatives for adipic acid production (Sikazwe et al., 2024), industrial wastewater for PHA biosynthesis (Saratale et al., 2024), rice bran for lactic acid and biogas generation (Herrmann et al., 2024), and palm oil refinery residues for the production of glycerin, lactic acid, and succinic acid (Gheewala et al., 2022). Consistent with these approaches, we investigated the potential of *E. coli* harboring pBSK-*CAB*$_{A\text{-}04}$ to utilize crude glycerol, a low-value byproduct of the biodiesel industry, as the sole carbon source for PHA production.

Please cite this article as: Pachimsawat J., Tsuge T., Napathorn S.C. Rewiring *Escherichia coli* central carbon metabolism for the sustainable bioconversion of waste glycerol into biodegradable polyhydroxybutyrate. Biofuel Research Journal 47 (2025) 2451-2469. DOI: 10.18331/BRJ2025.12.3.2.

Table 3.
Fermentation kinetics of PHB accumulation by *E. coli* K12-pBSK-$CAB_{A\text{-}04}$ cultivated at 30 °C using 20 g/L glucose as a sole carbon source at 24 h of cultivation varying inoculum concentration.

Inoculum Concentration	1%[1]	3%	5%	10%
Cell production				
Maximum CDM (g/L)	2.6 ± 0.2[a2]	3.5 ± 0.2[b]	3.5 ± 0.1[b]	3.2 ± 0.1[b]
Maximum CDM yeld (g CDM/g glucose)	0.16	0.16	0.14	0.12
Maximum RCM (g/L)	1.5 ± 0.2	1.5 ± 0.2	1.4 ± 0.1	1.4 ± 0.1
Maximum RCM yield (g RCM/g glucose)	0.2	0.2	0.1	0.1
PHB production				
Maximum PHB concentration (g/L)	1.1 ± 0.0[e]	1.9 ± 0.0[d]	2.1 ± 0.0[c]	1.8 ± 0.0[f]
Productivity (g/L.h)	0.05	0.08	0.09	0.07
Maximum PHB yield (g PHB/g glucose)	0.11	0.19	0.20	0.15
Maximum PHB content (wt%)	41.5 ± 0.8	55.5 ± 1.2	59.2 ± 0.7	56.2 ± 0.6

[1] Results are expressed as mean ± SD (n = 3).
[2] The different superscript letters within the same column are significantly different at $p < 0.05$.

Table 4.
Fermentation kinetics of PHB accumulation by *E. coli* K12-pBSK-$CAB_{A\text{-}04}$ cultivated at 37 °C using various concentrations of glucose as a sole carbon source and 5% inoculum concentration.

Glucose Concentration	10 g/L[1]	20 g/L	30 g/L	40 g/L
Maximum CDM (g/L)	2.9 ± 0.0[a2]	2.8 ± 0.2[a]	2.8 ± 0.1[a]	2.2 ± 0.2[b]
Maximum RCM (g/L)	2.1 ± 0.4	1.5 ± 0.2	1.5 ± 0.1	1.6 ± 0.1
Maximum RCM yield (g RCM/g glucose)	0.3	0.1	0.1	0.3
Maximum PHB concentration (g/L)	1.0 ± 0.0[e]	1.5 ± 0.1[d]	1.3 ± 0.0[d]	0.4 ± 0.0[e]
Productivity (g/L·h)	0.03	0.05	0.06	0.02
Maximum PHB yield (g PHB/g glucose)	0.10	0.12	0.11	0.08
Maximum PHB content (wt%)	38.7 ± 0.6	48.8 ± 3.4	48.2 ± 3.9	23.3 ± 1.8

[1] Results are expressed as mean ± SD (n = 3).
[2] The different superscript letters within the same column are significantly different at $p < 0.05$.

Extensive evidence indicates that traditional polymer production and waste management practices are unsustainable and have already caused significant, and in some cases irreversible, environmental harm (Chanprateep, 2010; Kookos et al., 2019). These concerns primarily stem

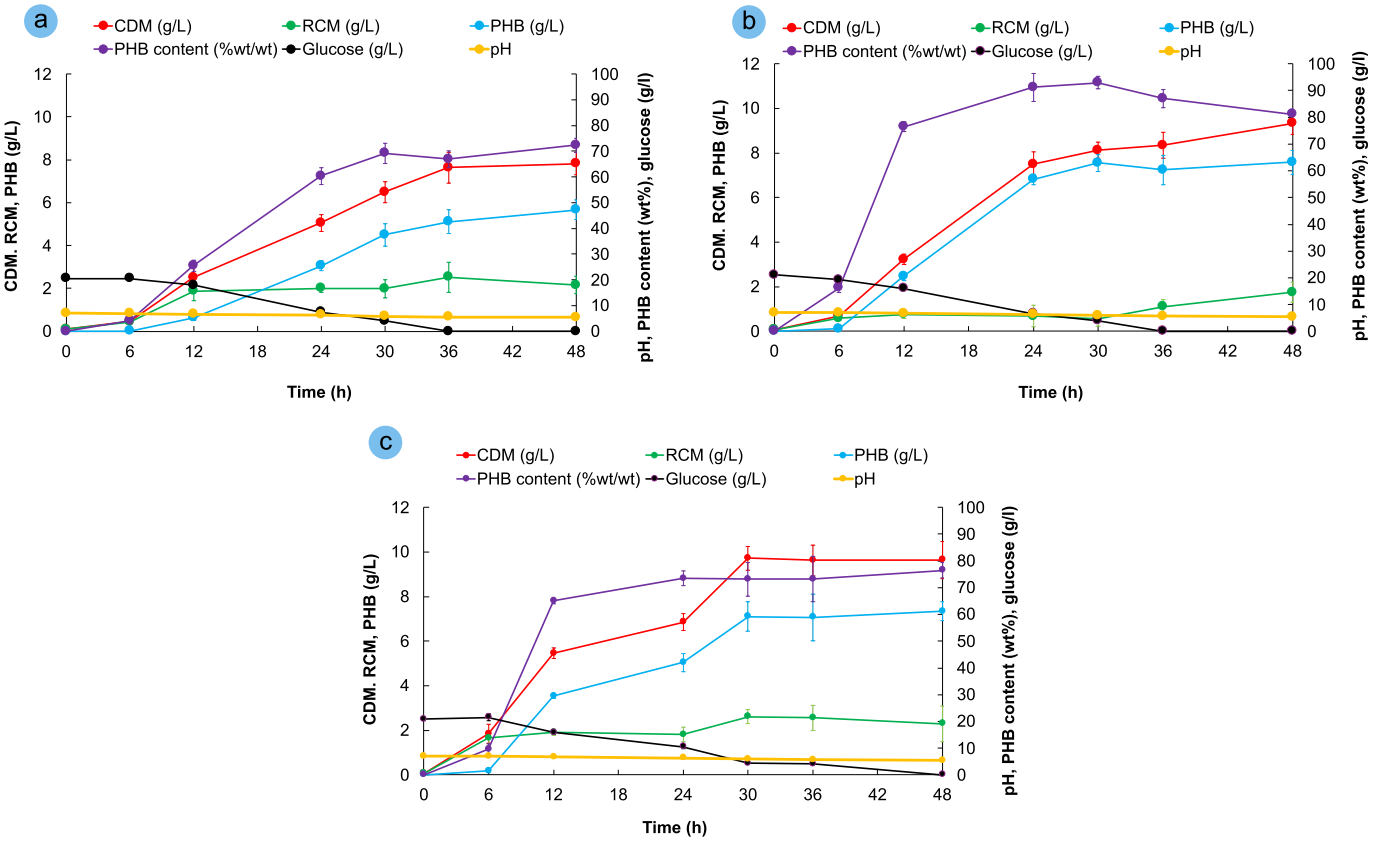

Fig.5. Time course of PHB production by recombinant *E. coli* **(a)** Δ*pgi*-pBSK-$CAB_{A\text{-}04}$, **(b)** Δ*edd*-pBSK-$CAB_{A\text{-}04}$, and **(c)** K12-pBSK-$CAB_{A\text{-}04}$ cultivated at 200 rpm and 30 °C for 48 h in LB medium supplemented with 20 g/L glucose as the sole carbon source for flask-scale production.

from the heavy reliance on fossil-based feedstocks and the environmental persistence of synthetic polymers. In response, increasing attention has been directed toward the production of biodegradable polymers such as PHB from renewable resources. However, early assessments of the environmental performance of PHB raised questions regarding its true sustainability (Goswami et al., 2023). Renouf et al. (2008) reported that

Please cite this article as: Pachimsawat J., Tsuge T., Napathorn S.C. Rewiring *Escherichia coli* central carbon metabolism for the sustainable bioconversion of waste glycerol into biodegradable polyhydroxybutyrate. Biofuel Research Journal 47 (2025) 2451-2469. DOI: 10.18331/BRJ2025.12.3.2.

Table 5.
Comparison of kinetic parameter, mechanical and thermal properties of PHB produced by recombinant *E. coli* strain Δ*edd*-pBSK-*CAB*$_{A-04}$, Δ*pgi*-pBSK-*CAB*$_{A-04}$ and K12-pBSK-*CAB*$_{A-04}$ at 48 h of cultivation.

	Recombinant *E. coli* Strain		
	Δ*edd*-pBSK-*CAB*$_{A-04}$	Δ*pgi*-pBSK-*CAB*$_{A-04}$	K12-pBSK-*CAB*$_{A-04}$
Maximum CDM (g/L)	9.3 ± 0.5	7.8 ± 0.5	9.7 ± 0.5
Maximum PHB concentration (g/L)	7.6 ± 0.5	5.7 ± 0.5	7.3 ± 0.4
Maximum PHB content (wt%)	93.0	72.4	76.5
Specific growth rate (1/h)	0.05	0.06	0.05
Specific production rate (g/g-RCM·h)	0.21	0.08	0.08
Specific consumption rate (g/g-RCM·h)	0.59	0.28	0.24
Productivity (g/L·h)	0.25	0.15	0.24
$\gamma_{x/s}$ (g CDM/ g carbon source)	0.04	0.08	0.10
$\gamma_{p/s}$ (g PHB/ g carbon source)	0.37	0.26	0.36
Ethanol concentrations (g/L)	1.6	2.0	1.7
M_w (Da)	2.9×10^5	1.5×10^5	7.7×10^5
M_n (Da)	1.8×10^5	7.9×10^4	5.0×10^5
PDI	1.6	2.0	1.5
T_g (°C)	4.2	4.0	5.2
T_c (°C)	46.7	52.6	42.1
T_m (°C)	172.2	173.4	177.1
ΔH_f (J/g)	105.5	99.0	99.0
%Xc	72.3	67.8	67.8
Young's Modulus (MPa)	459.0	353.8	294.6
Tensile strength (MPa)	10.2	4.7	3.3
Elongation at break (%)	3.0	1.3	0.6

monosaccharide production from sugarcane results in approximately 105 kg CO_2-eq/tonne and a net nonrenewable energy use (NREU) of −7,970 MJ/tonne, suggesting energy-saving potential. In contrast, corn-derived monosaccharides are associated with significantly greater environmental burdens, with estimated GHG emissions of 980 kg CO_2-eq/tonne and an NREU of 6,300 MJ/tonne. More recent studies provide additional insights (Renouf et al., 2008).

For example, Kachrimanidou et al. (2021) reported that PHB production from sunflower meal and crude glycerol, a byproduct of biodiesel production, can provide clear environmental advantages. In their study, the life cycle analysis (LCA) revealed greenhouse gas emissions of approximately 0.64 kg CO_2-eq/kg PHB and an abiotic depletion potential of 61.7 MJ/kg PHB, which are both lower than those of polypropylene. Notably, the highest energy demands were associated with the PHB production stage (27.9 MJ/kg), followed by contributions from crude glycerol (12.6 MJ/kg) and sunflower meal production (13.4 MJ/kg), largely due to steam, electricity, and fuel usage (Kachrimanidou et al., 2021). Similarly, Kookos et al. (2019) performed a detailed life cycle inventory and assessment of PHB production, concluding that key environmental indicators, including GHG emissions, NREU, acidification potential (AP), and eutrophication potential (EP), are highly dependent on both the renewable feedstock selected and the allocation methodology used. These findings explain the discrepancies among earlier studies and reinforce that, under optimized conditions, PHB production can be significantly more environmentally favorable than the production of petrochemical-based plastics. Furthermore, the incorporation of low-cost, renewable substrates such as agricultural residues or food industry byproducts, particularly within integrated biorefinery systems, enhances overall sustainability. Nevertheless, a comprehensive evaluation of PHB production must also address the economic and social dimensions, underscoring the need for continued interdisciplinary research to develop balanced sustainability frameworks and to identify technologies capable of supporting the transition to a circular bioeconomy (Kookos et al., 2019).

Therefore, we further evaluated the potential of *E. coli* strains harboring pBSK-*CAB*$_{A-04}$ to utilize an inexpensive carbon source, crude glycerol derived from the biodiesel industry, for PHB production. The composition of the crude glycerol used in this study was characterized and was found to contain 81.04% (w/w) glycerol, 0.004% (w/w) methanol, 13.5% (w/w) moisture, 3.31% (w/w) sodium chloride, 1.13% (w/w) ash, and 0.99% (w/w) material classified as nonglycerol organic matter (MONG), as reported previously (Phothong et al., 2024b). The performance of *E. coli* Δ*edd*-pBSK-*CAB*$_{A-04}$, Δ*pgi*-pBSK-*CAB*$_{A-04}$, and K12-pBSK-*CAB*$_{A-04}$ in PHB production using crude glycerol as the sole carbon source is summarized in **Table 6**. Interestingly, both *E. coli* Δ*edd*-pBSK-*CAB*$_{A-04}$ and Δ*pgi*-pBSK-*CAB*$_{A-04}$ presented a greater biomass and PHB concentrations than did the parental strain. After 24 h, recombinant *E. coli* Δ*edd*-pBSK-*CAB*$_{A-04}$ and Δ*pgi*-pBSK-*CAB*$_{A-04}$ accumulated 3.7±0.1 and 3.5±0.2 g/L PHB with 74.8±1.4 and 62.0±1.1 wt% PHB contents, respectively. The PHB content of the parental strain K12 was 1.1±0.1 g/L, with a PHB content of 48.6±0.8 wt%. This result suggested that the metabolic perturbations caused by the deletion of the *edd* and *pgi* genes likely had a positive effect on PHB production from crude glycerol.

Generally, the valorization of crude glycerol results in lower yields due to the low content of glycerol and the presence of impurities such as methanol, ash, salts, and heavy metals from the transesterification of biodiesel. These impurities can negatively affect microbial growth and product formation. According to Bennett et al. (2021), the growth of *E. coli* was inhibited at a 1 M methanol concentration and completely inhibited at a 1.5 M methanol concentration. Since the crude glycerol used in this research contained less than 0.005% methanol, we assumed that the crude glycerol components had no inhibitory effects, as described in our previous studies (Boontip et al., 2021; Phothong et al., 2024b). A comparative analysis of PHB production by various previously reported microbial strains is presented in **Table 7**.

3.4. PHB production by E. coli Δedd-pBSK-CAB$_{A-04}$ from glucose in a 5-L fermenter

Scaled-up cultivation for PHB production was conducted in a 5-L fermenter, and the time courses of cell growth and PHB accumulation are presented in **Figure 6**. The CDM and RCM of *E. coli* Δ*edd*-pBSK-*CAB*$_{A-04}$ after 24 h were 5.60±0.21 and 3.38±0.19 g/L, respectively. At 54 h, CDM remained relatively unchanged at 5.63±0.29 g/L, whereas RCM decreased to 1.85±0.11 g/L. This result suggests a significant accumulation of PHB in

Please cite this article as: Pachimsawat J., Tsuge T., Napathorn S.C. Rewiring *Escherichia coli* central carbon metabolism for the sustainable bioconversion of waste glycerol into biodegradable polyhydroxybutyrate. Biofuel Research Journal 47 (2025) 2451-2469. DOI: 10.18331/BRJ2025.12.3.2.

Table 6.
Comparison of PHB production by recombinant *E. coli* strain Δ*edd*-pBSK-CAB_{A-04}, Δ*pgi*-pBSK-CAB_{A-04} and K12-pBSK-CAB_{A-04} cultivated in LB medium supplemented with either 20 g/L glucose or 20 g/L crude glycerol as a sole carbon source.

E. coli Strain	Carbon Source	Time (h)	CDM (g/L)	PHB Concentration (g/L)	PHB Content (wt%)
Δ*edd*	Glucose	24	7.5 ± 0.5	6.8 ± 0.2	91.2 ± 5.2
		48	9.3 ± 0.5	7.6 ± 0.5	81.1 ± 0.5
	Crude glycerol	24	3.7 ± 0.1	2.7 ± 0.1	74.8 ± 1.4
		48	4.9 ± 0.1	3.8 ± 0.0	76.9 ± 0.3
Δ*pgi*	Glucose	24	5.1 ± 0.4	3.1 ± 0.2	60.3 ± 3.2
		48	7.8 ± 0.5	5.7 ± 0.5	72.4 ± 2.7
	Crude glycerol	24	3.5 ± 0.2	2.2 ± 0.0	62.0 ± 1.1
		48	5.5 ± 0.1	3.4 ± 0.1	61.9 ± 1.9
K12	Glucose	24	6.9 ± 0.4	5.0 ± 0.4	73.5 ± 2.8
		48	9.6 ± 0.8	7.3 ± 0.4	76.5 ± 2.9
	Crude glycerol	24	2.2 ± 0.3	1.1 ± 0.0	48.6 ± 0.8
		48	3.4 ± 0.1	1.9 ± 0.0	55.8 ± 0.9

Table 7.
Comparison of PHB production using glucose as carbon source by recombinant microorganisms.

Strain	Strain Characteristics	Carbon Source	Condition	CDW (g/L)	PHB (wt%)	Ref.
C. necator A-04	Native strain	Fructose	30°C, 60 h	7.4 ± 1.5	78.4 ± 1.9	Napathorn (2021)
E. coli JM109	Harboring cold-shock inducible promoter of phaCAB from *C. necator* strain A-04	Glucose	37°C, 18 h	7.9 ± 0.7	89.8 ± 2.3	Boontip et al. (2021)
E. coli S17-1	Harboring cascaded P_{vgb} repeats and phaCAB from *C. necator*	Glucose	37°C, 48 h	6.30	91	Wu et al. (2014)
E. coli DH5α	Harboring pGETS109-*pha*	Glucose	30°C, 72 h	11.2 ± 0.1	57 ± 1.6	Hiroe et al. (2012)
E. coli JM109	Harboring pBAD/Thio-TOPO-phaCAB from *C. necator* strain A-04	Glucose	37°C, 24 h	6.1 ± 1.1	93.3 ± 0.9	Napathorn et al. (2021)
E. coli Δ*edd*-pBSK-CAB_{A-04}	Harboring phaCAB from *C. necator* strain A-04	Glucose	30°C, 24 h	7.5 ± 0.5	91.2 ± 5.2	**This Study**
E. coli Δ*pgi*-pBSK-CAB_{A-04}	Harboring phaCAB from *C. necator* strain A-04	Glucose	30°C, 48 h	7.8 ± 0.5	72.4 ± 2.7	**This Study**
E. coli K12-pBSK-CAB_{A-04}	Harboring phaCAB from *C. necator* strain A-04	Glucose	30°C, 24 h	6.9 ± 0.4	73.5 ± 2.8	**This Study**
Recombinant *R. glutinis*	Harboring codon-optimized towards phaCAB from *C. necator*	Crude glycerol	24°C, 48 h	4.6	62	Aristya et al. (2022)
E. coli JM109	Harboring pUC19-23119phaCAB$_{A-04}$	Crude glycerol	30°C, 24 h	4.4 ± 0.3	7.4 ± 0.8	Phothong et al. (2024b)
E. coli BL21 (DE3)	Harboring *phaA* and *phaB* from *C. necator* and *phaC* from *A. hydrophila*	Crude glycerol	37°C, 24 h	4.0 ± 0.4	13.9 ± 2.5	Phithakrotchanakoon et al. (2014)
E. coli Δ*edd*-pBSK-CAB_{A-04}	Harboring phaCAB from *C. necator* strain A-04	Crude glycerol	30°C, 24 h	3.7 ± 0.1	74.8 ± 1.4	**This Study**
E. coli Δ*pgi*-pBSK-CAB_{A-04}	Harboring phaCAB from *C. necator* strain A-04	Crude glycerol	30°C, 48 h	5.5 ± 0.1	61.9 ± 1.9	**This Study**
E. coli K12-pBSK-CAB_{A-04}	Harboring phaCAB from *C. necator* strain A-04	Crude glycerol	30°C, 48 h	3.4 ± 0.1	55.8 ± 0.9	**This Study**

the cells, reaching a maximum PHB concentration of 3.78±0.18 g/L and a content of 67.1±3.1% (w/w) at 54 h. However, compared with shaker flask cultivation (**Fig. 5**), substantial decreases in both the biomass and PHB production were observed in the fermenter. This inconsistency may be attributed to several factors, including vector instability, a high cell density, and challenges associated with scale-up parameters. One key issue appears to be plasmid instability during fermentation. Despite pBSK being a high-copy-number plasmid (approximately 500–700 copies), segregation instability remains a significant concern under large-scale cultivation (Škulj et al., 2008). Plasmid-free cells can rapidly accumulate, reducing overall productivity, as evidenced in **Figure 6**. Plasmid stability, measured as the relative plasmid retention in *E. coli* Δ*edd*-pBSK-CAB_{A-04} over time, is presented in **Figure 7** to validate the plasmid instability observed in this study.

Several strategies for strain stabilization can be employed to address this challenge and improve industrial viability. One effective approach is the chromosomal integration of the *phaCAB* operon into the *E. coli* genome, which eliminates the dependence on plasmid-based systems and ensures genetic stability during long-term fermentation. This strategy also avoids the need for antibiotic selection, thereby reducing production costs and aligning with regulatory standards for industrial use (Tyo et al., 2009). Another method involves the incorporation of toxin–antitoxin systems, such as the *hok/sok* or *ccdAB* modules, which selectively eliminate plasmid-free cells and help maintain plasmid stability without the use of antibiotics (Jurėnas et al., 2022). Additionally, stable shuttle vectors such as pWB980, which exhibit high copy numbers and robustness across hosts such as *E. coli* and *Bacillus subtilis*, can be utilized to improve the reliability of expression (Zhao et al., 2020). Furthermore, CRISPR–Cas genome editing

Please cite this article as: Pachimsawat J., Tsuge T., Napathorn S.C. Rewiring *Escherichia coli* central carbon metabolism for the sustainable bioconversion of waste glycerol into biodegradable polyhydroxybutyrate. Biofuel Research Journal 47 (2025) 2451-2469. DOI: 10.18331/BRJ2025.12.3.2.

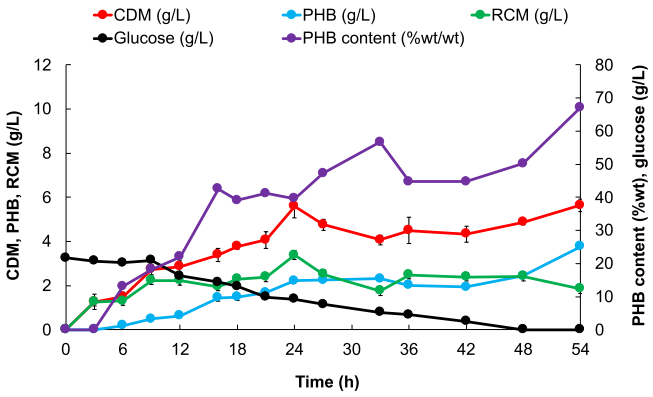

Fig. 6. Time course of PHB production by the recombinant *E. coli* strain Δ*edd*-pBSK-*CAB*$_{A-04}$ cultivated at 30 °C in LB medium supplemented with 20 g/L glucose as the sole carbon source in a 10-L fermenter.

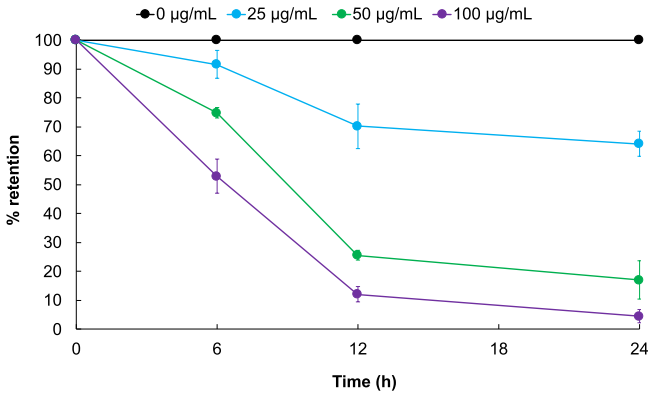

Fig. 7. The results of the plasmid stability test are presented as the relative plasmid retention in *E. coli* Δ*edd* over time. Each experiment was repeated three times, and the mean values with standard deviations (error bars) are presented.

technologies are precise tools for integrating and optimizing biosynthetic pathways directly into chromosomes, thereby increasing strain stability, metabolic efficiency, and the overall yields of PHB and other biopolymers (Wei and Li, 2023). Collectively, these strategies represent promising solutions for improving the genetic stability and scalability of engineered strains, thus increasing their suitability for industrial-scale bioplastic production.

While this study demonstrated the benefits of *E. coli* Δ*edd*-pBSK-*CAB*$_{A-04}$ in increasing PHB production and utilizing cost-effective feedstocks, the potential drawbacks associated with plasmid-based overexpression and metabolic pathway rewiring must be recognized. A significant concern is the metabolic burden imposed by the high-level expression of heterologous genes, which can reduce cellular fitness, slow growth rates, and lead to plasmid instability during extended cultivation. Moreover, the deletion of the *edd* gene disrupts the ED pathway, potentially inducing a redox imbalance, especially affecting NADPH/NADP$^+$ homeostasis—an essential factor for PHB biosynthesis and other NADPH-dependent metabolic processes (Alkotaini et al., 2018; Ling et al., 2018; Chen et al., 2024). Under oxygen-limited or industrial-scale conditions, such imbalances may constrain cofactor availability or redirect carbon fluxes in undesirable ways. Additionally, overflow metabolism can result in the accumulation of inhibitory byproducts such as acetate and lactate, further impacting cell viability and product yield. These limitations are particularly relevant in large-scale bioprocesses, where a reduced selective pressure for plasmid maintenance and suboptimal oxygen transfer can exacerbate genetic instability and metabolic stress (Alkotaini et al., 2018).

3.5. Molecular weight distribution and thermal properties of the PHB film

Mechanical properties of PHB polymers extracted from *E. coli* Δ*edd*-pBSK-*CAB*$_{A-04}$, Δ*pgi*-pBSK-*CAB*$_{A-04}$, and K12-pBSK-*CAB*$_{A-04}$ were analyzed by Universal Testing Machine. Young's Modulus, tensile strength, and elongation at break of these films are illustrated in **Table 5**. The result showed that PHB film produced by K12-pBSK-*CAB*$_{A-04}$ gave the lowest Young's modulus, tensile strength, and elongation at break, with the values of 295 MPa, 3.3 MPa, and 0.6% respectively. Higher values were observed in the PHB film produced by *E. coli* Δ*edd*-pBSK-*CAB*$_{A-04}$ and Δ*pgi*-pBSK-*CAB*$_{A-04}$. PHB film from *E. coli* Δ*edd*-pBSK-*CAB*$_{A-04}$ had the highest Young's modulus, tensile strength, and elongation at break, with the values of 459 MPa, 10.2 MPa, and 3.0% respectively. The PHB film produced from *E. coli* Δ*pgi*-pBSK-*CAB*$_{A-04}$ had its Young's modulus, tensile strength, and elongation at break of 354 MPa, 4.7 MPa, and 1.3%, respectively. The mechanical properties of PHB in this study indicated a lower value of Young's Modulus, compared to typical PHB, which has a high value of Young's Modulus, making the polymer stiff and brittle. The differences in mechanical properties observed in this study may be affected by several factors, such as the degree of amorphism, purity of PHB, and environmental conditions (Attallah et al., 2021).

The molecular weights of PHB polymers extracted from *E. coli* Δ*edd*-pBSK-*CAB*$_{A-04}$, Δ*pgi*-pBSK-*CAB*$_{A-04}$, and K12-pBSK-*CAB*$_{A-04}$ were analyzed by gel permeation chromatography (GPC). The number average molecular weight (M_n), weight average molecular weight (M_w), and PDI of these PHB films are presented in **Table 5**. The results showed that the PHB film produced by K12-pBSK-*CAB*$_{A-04}$ had the highest M_w and M_n values of 7.7×10^5 and 5.1×10^5 Da, respectively. In contrast, the M_w and M_n values of the PHB film produced by *E. coli* Δ*edd*-pBSK-*CAB*$_{A-04}$ were 2.9×10^5 and 1.8×10^5 Da, respectively.

The PHB film produced by *E. coli* Δ*pgi*-pBSK-*CAB*$_{A-04}$ presented the lowest M_w and M_n values of 1.5×10^5 and 7.9×10^4 Da, respectively. These results indicated that *E. coli* Δ*edd*-pBSK-*CAB*$_{A-04}$ and Δ*pgi*-pBSK-*CAB*$_{A-04}$ produced lower-molecular-weight PHB than did K12-pBSK-*CAB*$_{A-04}$. The molecular weight of PHB has been reported to be in the range of 0.1×10^6 to 2×10^6 Da (Tsuge, 2016). To date, the precise mechanism of PHA monomer elongation is still unclear. The decrease in the molecular weight of PHB produced by *E. coli* Δ*edd*-pBSK-*CAB*$_{A-04}$ and Δ*pgi*-pBSK-*CAB*$_{A-04}$ compared with K12-pBSK-*CAB*$_{A-04}$ could be explained by several mechanisms. First, the molecular weight changed due to PHA synthase (phaC) activity. The disruptions of the EDP and EMP in *E. coli* Δ*edd*-pBSK-*CAB*$_{A-04}$ and Δ*pgi*-pBSK-*CAB*$_{A-04}$ altered the flux of carbon through the PPP with the aim of producing greater amounts of NADPH, incorporating and increasing PHA production. NADPH is known as the main bottleneck in PHA production to generate 3-hydroxybutyryl-CoA, the main precursor for PhaC. Providing available NADPH may lead to an increase in phaC activity. Thus, *E. coli* Δ*edd*-pBSK-*CAB*$_{A-04}$ and Δ*pgi*-pBSK-*CAB*$_{A-04}$ might have greater phaC activity than K12-pBSK-*CAB*$_{A-04}$. Many researchers have reported that the molecular weight of PHA decreases with increasing PHA synthase activity (Sim et al., 2001; Tsuge, 2016).

Another possible explanation for the decrease in the molecular weight of PHB produced by *E. coli* Δ*edd*-pBSK-*CAB*$_{A-04}$ and Δ*pgi*-pBSK-*CAB*$_{A-04}$ is the formation of ethanol, which may inhibit the polymerization of PHA chains (Rangel et al., 2023). When glucose is used as the sole carbon source, the theoretical yields of ethanol production differ depending on the metabolic pathway. According to Seol et al. (2014), glucose metabolism *via* the EMP pathway produces 2 H_2, 1 ethanol, and 2 ATP molecules per glucose molecule. The pentose phosphate pathway (PPP) yields 1.67 H_2, 1.67 ethanol, and 1.67 ATP molecules, whereas the Entner–Doudoroff pathway (EDP) results in 2 H_2, 1 ethanol, and 1 ATP molecules per glucose molecule (Seol et al., 2014). Given that *E. coli* Δ*edd*-pBSK-*CAB*$_{A-04}$ and Δ*pgi*-pBSK-*CAB*$_{A-04}$ redirected carbon flux predominantly through the PPP, their theoretical ethanol yields were maximized at 1.67 mol of ethanol per mol of glucose. Based on this evidence and the data in **Table 5**, we conclude that ethanol production by *E. coli* Δ*edd*-pBSK-*CAB*$_{A-04}$ and Δ*pgi*-pBSK-*CAB*$_{A-04}$ was higher than that by K12-pBSK-*CAB*$_{A-04}$.

In support of this hypothesis, Seol et al. (2014) experimentally showed that an EMP-disrupted strain presented an ethanol yield of 0.95 mol/mol glucose, whereas the ethanol yield of the parental strain was 0.84 mol/mol. Ethanol is a known chain transfer agent that can covalently bind to the carboxyl terminus of the growing PHA chain, thereby

Please cite this article as: Pachimsawat J., Tsuge T., Napathorn S.C. Rewiring *Escherichia coli* central carbon metabolism for the sustainable bioconversion of waste glycerol into biodegradable polyhydroxybutyrate. Biofuel Research Journal 47 (2025) 2451-2469. DOI: 10.18331/BRJ2025.12.3.2.

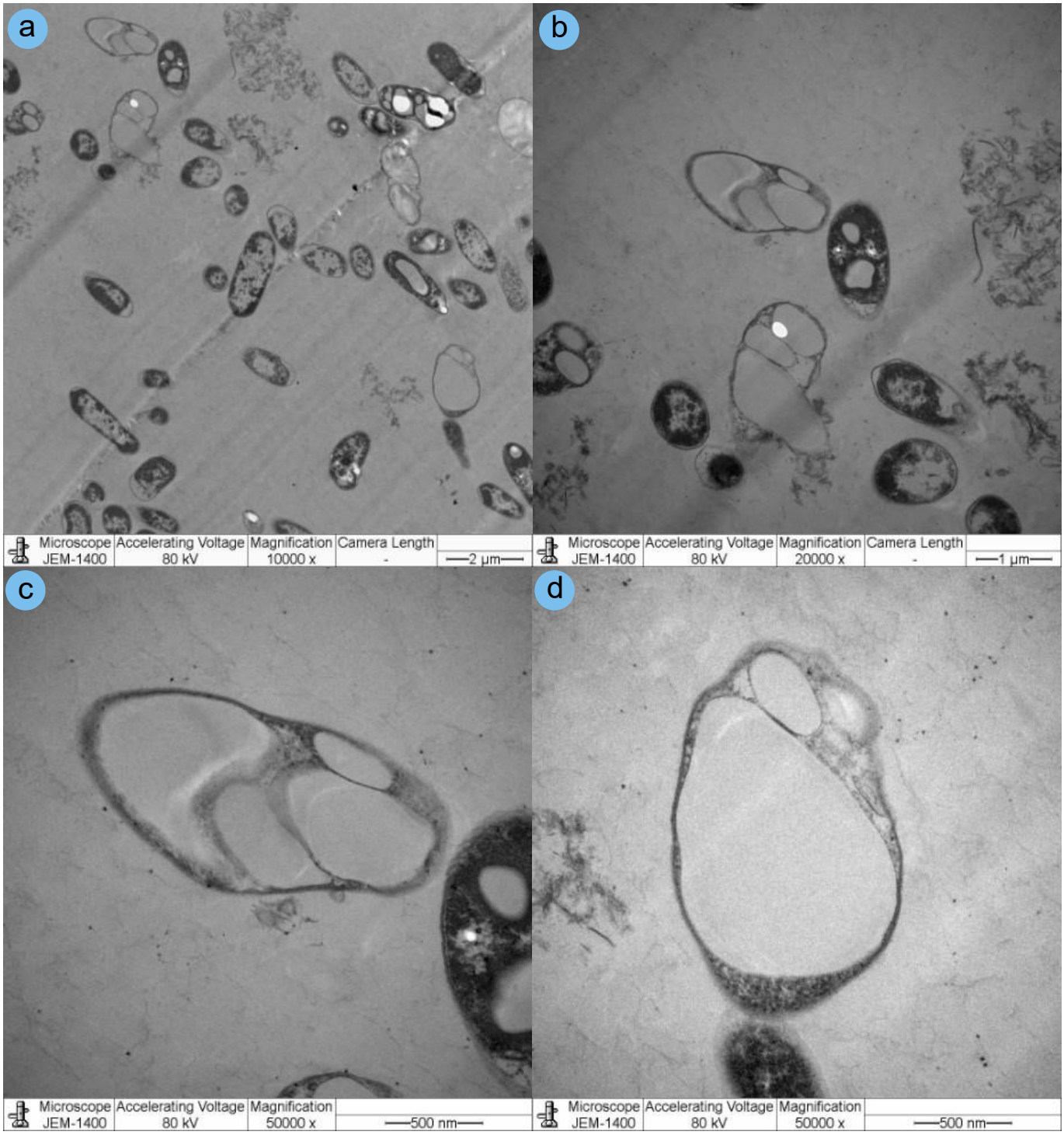

Fig. 8. TEM images at magnifications of **(a)** 10000×, **(b)** 20000×, **(c)** 50000×, and **(d)** 50000× of the morphology of the *E. coli* strain Δ*edd*-pBSK-$CAB_{A\text{-}04}$ and PHB granules after cultivation at 30 °C in LB medium supplemented with 20 g/L glucose as the sole carbon source for 48 h.

terminating polymerization and resulting in lower-molecular-weight polymers (Tsuge, 2016). This hypothesis is further supported by Hiroe et al. (2015), who reported a reduction in the molecular weight of PHB when ethanol was supplemented externally during cultivation (Hiroe et al., 2015). Therefore, elevated ethanol production in *E. coli* Δ*edd*-pBSK-$CAB_{A\text{-}04}$ and Δ*pgi*-pBSK-$CAB_{A\text{-}04}$ plausibly interferes with PHB chain elongation, ultimately leading to the lower molecular weights observed in these strains than in the parental *E. coli* K12-pBSK-$CAB_{A\text{-}04}$ strain. Experimental quantification of residual ethanol concentrations in the culture medium would be valuable to strengthen this claim and is currently under consideration for future work.

The effects of rewiring *E. coli* central carbon metabolism *via* Δ*edd* and Δ*pgi* deletions on the thermal properties of the produced PHB were evaluated and compared with those of *E. coli* K12-pBSK-$CAB_{A\text{-}04}$. The

Please cite this article as: Pachimsawat J., Tsuge T., Napathorn S.C. Rewiring *Escherichia coli* central carbon metabolism for the sustainable bioconversion of waste glycerol into biodegradable polyhydroxybutyrate. Biofuel Research Journal 47 (2025) 2451-2469. DOI: 10.18331/BRJ2025.12.3.2.

thermal properties of PHB produced by *E. coli* Δ*edd*-pBSK-*CAB*$_{A-04}$, Δ*pgi*-pBSK-*CAB*$_{A-04}$, and K12-pBSK-*CAB*$_{A-04}$ were analyzed using differential scanning calorimetry (DSC), as summarized in **Table 5**. All PHB samples exhibited a single melting temperature (T_m) in the first heating cycle, with values ranging from 178–183 °C. During the second heating cycle, the melting temperature decreased slightly, ranging from 172–177 °C. The glass transition temperature (T_g) and crystallization temperature (T_c) were found to be between 4 and 5 °C and between 42 and 53 °C, respectively. The percent crystallinity of PHB produced by *E. coli* Δ*pgi*-pBSK-*CAB*$_{A-04}$ was similar to that of the parental strain at approximately 67.8%. Notably, the PHB produced by *E. coli* Δ*edd*-pBSK-*CAB*$_{A-04}$ presented an increased percent crystallinity of 72.3%, suggesting that the Δ*edd* mutation may increase the degree of polymer chain ordering and packing in the resulting PHB (Garcia-Garcia et al., 2022; Sinsukudomchai et al., 2023).

3.6 PHB granule observation by TEM

E. coli Δ*edd*-pBSK-*CAB*$_{A-04}$ was cultivated for 48 h, and PHB granules were visualized using transmission electron microscopy (TEM), as shown in **Figure 8**. The PHB granules appeared as electron-transparent (white) inclusions within the cytoplasm, whereas the bacterial cells were observed in varying shades of gray, with overall dimensions ranging from 1–3 µm in length and approximately 1 µm in diameter. Each cell typically contained 1 to 3 major PHB granules, with the most frequent granule diameter ranging from 0.1–1.6 µm (**Fig. 9**). The average size of the cell and the PHB granule was 1.4 and 0.3 µm^2, respectively. In comparison, the diameters of PHB granules in *C. necator* strain A-04 and most other PHB-accumulating bacteria are generally within the range of 0.2–0.5 µm (Jendrossek et al., 2007; Chanprateep et al., 2008). Thus, the PHB granules observed in *E. coli* Δ*edd*-pBSK-*CAB*$_{A-04}$ were slightly larger than those typically reported in other bacterial species (Jendrossek et al., 2007), suggesting potential differences in granule formation or regulatory mechanisms in the engineered strain. Previous studies have reported a positive correlation between cell size and PHB granule size, indicating that larger cells tend to contain larger PHB granules, as reflected by the slopes shown in **Figure 9** (Tian et al., 2005; Chen et al., 2025).

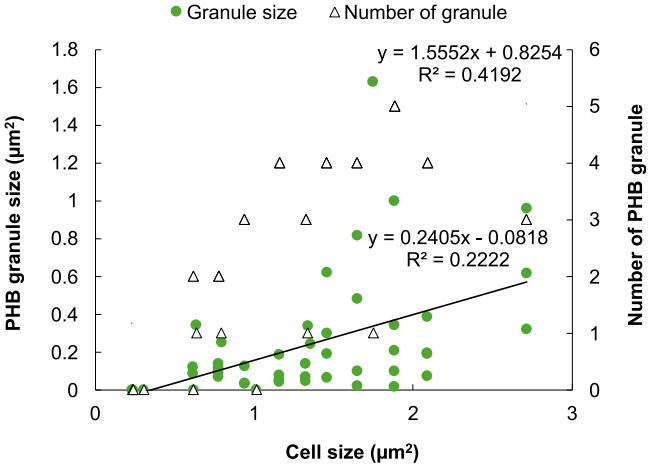

Fig. 9. The dependency of the PHB granule size (black circle) and the number of PHB granules per cell (white upward-pointing triangle) on the whole-cell size in a population of *E. coli* Δ*edd*-pBSK-*CAB*$_{A-04}$ cultivated at 30 °C in LB medium supplemented with 20 g/L glucose as the sole carbon source for 48 h. Both straight lines represent the best-fitting lines for the relationship between the granule size and the cell size, drawn with (straight line) and without (broken line), forced to the origin of the coordinate system. The origin included a straight line that refers to the assumption that PHB granules grow in parallel with cellular growth. The data were obtained by an ImageJ area analysis of binary rearranged TEM images.

In some cells, signs of autolysis and the extracellular secretion of PHB were observed. Notably, certain bacterial cells did not accumulate intracellular PHB, despite the gas chromatography analysis indicating a PHB content of 81.1% (w/w). This discrepancy may be attributed to plasmid segregation instability during cell division, as previously reported (Škulj et al., 2008). These observations align with the findings presented in *Section 3.4*, where the reduced PHB concentration and content in the 5-L fermenter were linked to plasmid instability. Furthermore, the TEM images revealed the presence of numerous small vesicles clustered around the periphery of the bacterial cells, which may be associated with vesicle-mediated transport or membrane remodeling during PHB synthesis.

4. Conclusions and future research directions

Metabolic engineering of *E. coli* through the deletion of the *edd* gene offers broader control over cellular metabolism, enabling a more precise redirection of carbon flux. In this study, we demonstrated that *E. coli* Δ*edd* strains adapted their growth profile and carbon utilization pathways when cultivated on glucose. Although the *edd*-deficient strain presented a slower growth rate than the parental strain, the incorporation of the PHA biosynthetic pathway not only restored bacterial growth but also significantly increased PHB accumulation. The engineered strain *E. coli* Δ*edd*-pBSK-*CAB*$_{A-04}$ achieved PHB contents of 91.2 wt% and 74.8 wt% within 24 h of cultivation at 30 °C in LB medium supplemented with 20 g/L glucose and crude glycerol, respectively. The ability of this strain to utilize crude glycerol, a low-cost byproduct of the biodiesel industry, as the sole carbon source indicates its economic potential for scale-up and its applicability in circular bioeconomy initiatives. Moreover, this strategy highlights the valorization of industrial waste as a viable and sustainable feedstock in microbial bioprocesses. In addition to PHB, the Δ*edd* strain shows potential as a versatile microbial chassis for the production of other NADPH-dependent compounds, such as amino acids, lycopene, isoprenoids, and vitamins.

Future research should focus on optimizing the scale-up of PHB production by *E. coli* Δ*edd*-pBSK-*CAB*$_{A-04}$. The parameters, including dissolved oxygen levels, substrate concentrations, antibiotic supplementation, and agitation rates, should be optimized in batch fermentation. High-cell-density cultivation strategies, such as fed-batch and continuous fermentation, should be developed based on these optimized conditions. Additionally, the production of other members of the PHA family, such as P(3HB-*co*-3HV) and P(3HB-*co*-4HB), from crude glycerol should be explored to further leverage waste valorization. Preliminary experiments confirmed the potential to produce P(3HB-*co*-3HV) containing 12–41 mol% 3HV by cosupplementing the medium with structurally related carbon sources such as sodium propionate alongside glucose or crude glycerol.

Acknowledgments

E. coli strains *Δpgi* and *Δedd* were obtained from National BioResource Project (NIG, Japan): *E. coli*. The authors greatly appreciate Professor Watanalai Panbangred (Department of Biotechnology, Faculty of Science, Mahidol University, Bangkok, Thailand) for providing *E. coli* K12. This research was supported by the 100th Anniversary Chulalongkorn University Fund for Doctoral Scholarship (GCUGE11), the 90th Anniversary of Chulalongkorn University Scholarship (GCUGR1125621033D), and the Overseas Research Experience Scholarship for Graduate Student Scholarship (GCUGR18). This research was also funded by the Thailand Science Research and Innovation Fund, Chulalongkorn University (BCG_FF_68_249_2300_058).

Author Contributions

Jittakan Pachimsawat: Methodology, Formal analysis, Investigation, Discussion, Writing—original draft. **Takeharu Tsuge:** Methodology, Discussion, Supervision. **Suchada Chanprateep Napathorn:** Conceptualization, Methodology, Visualization, Supervision, Discussion, Project administration, Funding acquisition, Resources, Writing—original draft, Writing—review and editing. All the authors read and approved the final version of the manuscript.

Conflict of interest

The authors declare that they have no conflicts of interest to disclose.

Please cite this article as: Pachimsawat J., Tsuge T., Napathorn S.C. Rewiring *Escherichia coli* central carbon metabolism for the sustainable bioconversion of waste glycerol into biodegradable polyhydroxybutyrate. Biofuel Research Journal 47 (2025) 2451-2469. DOI: 10.18331/BRJ2025.12.3.2.

References

[1] Ahn, J., Chung, B.K., Lee, D.Y., Park, M., Karimi, I.A., Jung, J.K., Lee, H., 2011. NADPH-dependent pgi-gene knockout Escherichia coli metabolism producing shikimate on different carbon sources. FEMS Microbiol. Lett. 324(1), 10-16.

[2] Akkoyunlu, B., Gabarre, C., Daly, S., Casey, E., Syron, E., 2024. Process modelling for industrial scale polyhydroxybutyrate production using fructose, formic acid and CO_2: assessing carbon sources and economic viability. Bioresour. Technol. 393, 130139.

[3] Alkotaini, B., Abdellaoui, S., Hasan, K., Grattieri, M., Quah, T., Cai, R., Yuan, M., Minteer, S.D., 2018. Sustainable bioelectrosynthesis of the bioplastic polyhydroxybutyrate: overcoming substrate requirement for NADH regeneration. ACS Sustainable Chem. Eng. 6(4), 4909-4915.

[4] Aristya, G.R., Lin, Y.J., Chang, J.S., Chang, J.J., Yen, H.W., 2022. Polyhydroxybutyrate (PHB) production from crude glycerol by genetic engineering of *Rhodotorula glutinis*. Bioresour. Technol. Rep. 18, 101048.

[5] Attallah, O.A., Mojicevic, M., Garcia, E.L., Azeem, M., Chen, Y., Asmawi, S., Brenan Fournet, M., 2021. Macro and micro routes to high performance bioplastics: bioplastic biodegradability and mechanical and barrier properties. Polymers. 13(13), 2155.

[6] Baba, T., Ara, T., Hasegawa, M., Takai, Y., Okumura, Y., Baba, M., Datsenko, K.A., Tomita, M., Wanner, B.L., Mori, H., 2006. Construction of Escherichia coli K-12 in-frame, single-gene knockout mutants: the Keio collection. Mol. Syst. Biol. 2, 2006.0008.

[7] Barham, P.J., Keller, A., Otun, E.L., Holmes, P.A., 1984. Crystallization and morphology of a bacterial thermoplastic: poly-3-hydroxybutyrate. J. Mater. Sci. 19(9), 2781-2794.

[8] Bennett, R.K., Dillon, M., Gerald Har, J.R., Agee, A., von Hagel, B., Rohlhill, J., Antoniewicz, M.R., Papoutsakis, E.T., 2020. Engineering Escherichia coli for methanol-dependent growth on glucose for metabolite production. Metab. Eng. 60, 45-55.

[9] Bennett, R.K., Gregory, G.J., Gonzalez, J.E., Har, J.R.G., Antoniewicz, M.R., Papoutsakis, E.T., 2021. Improving the methanol tolerance of an Escherichia coli methylotroph via adaptive laboratory evolution enhances synthetic methanol utilization. Front. Microbiol. 12, 638426.

[10] Bhuyan, S., Yadav, M., Giri, S.J., Begum, S., Das, S., Phukan, A., Priyadarshani, P., Sarkar, S., Jayswal, A., Kabyashree, K., Kumar, A., Mandal, M., Ray, S.K., 2023. Microliter spotting and micro-colony observation: a rapid and simple approach for counting bacterial colony forming units. J. Microbiol. Methods. 207, 106707.

[11] Boontip, T., Waditee-Sirisattha, R., Honda, K., Napathorn, S.C., 2021. Strategies for poly (3-hydroxybutyrate) production using a cold-shock promoter in Escherichia coli. Front. Bioeng. Biotechnol. 478.

[12] Canonaco, F., Hess, T.A., Heri, S., Wang, T., Szyperski, T., Sauer, U., 2001. Metabolic flux response to phosphoglucose isomerase knock-out in Escherichia coli and impact of overexpression of the soluble transhydrogenase UdhA. FEMS Microbiol. Lett. 204(2), 247-252.

[13] Chanprateep, S., 2010. Current trends in biodegradable polyhydroxyalkanoates. J. Biosci. Bioeng. 110(6), 621-632.

[14] Chanprateep, S., Katakura, Y., Visetkoop, S., Shimizu, H., Kulpreecha, S., Shioya, S., 2008. Characterization of new isolated Ralstonia eutropha strain A-04 and kinetic study of biodegradable copolyester poly (3-hydroxybutyrate-co-4-hydroxybutyrate) production. J. Ind. Microbiol. Biotechnol. 35(11), 1205-1215.

[15] Chanprateep, S., Kulpreecha, S., 2006. Production and characterization of biodegradable terpolymer poly (3-hydroxybutyrate-co-3-hydroxyvalerate-co-4-hydroxybutyrate) by Alcaligenes sp. A-04. J. Biosci. Bioeng.101(1), 51-56.

[16] Charusanti, P., Conrad, T.M., Knight, E.M., Venkataraman, K., Fong, N.L., Xie, B., Gao, Y., Palsson, B.O., 2010. Genetic basis of growth adaptation of Escherichia coli after deletion of pgi, a major metabolic gene. PLoS Genet. 6(11), e1001186.

[17] Chen, L., Xing, X., Zhang, P., Chen, L., Pei, H., 2024. Homeostatic regulation of NAD (H) and NADP (H) in cells. Genes Diseases. 11(5), 101146.

[18] Chen, Y.L., Liu, X., Zhang, L.Z., Yang, J.S., Guo, W.K., Zheng, S., Wang, J.L., Wu, F.Q., Yan, X., Wu, Q., 2025. Cell sizes matter for industrial bioproduction, a case of polyhydroxybutyrate. Adv. Sci. 12(14), 2412256.

[19] Favaro, L., Basaglia, M., Casella, S., 2019. Improving polyhydroxyalkanoate production from inexpensive carbon sources by genetic approaches: a review. Biofuels Bioprod. Biorefin. 13(1), 208-227.

[20] Fuhrman, L.K., Wanken, A., Nickerson, K.W., Conway, T., 1998. Rapid accumulation of intracellular 2-keto-3-deoxy-6-phosphogluconate in an Entner-Doudoroff aldolase mutant results in bacteriostasis. FEMS Microbiol. Lett. 159(2), 261-266.

[21] Garcia-Garcia, D., Quiles-Carrillo, L., Balart, R., Torres-Giner, S., Arrieta, M.P., 2022. Innovative solutions and challenges to increase the use of Poly (3-hydroxybutyrate) in food packaging and disposables. Eur. Polym. J. 178, 111505.

[22] Gebauer, B., Jendrossek, D., 2006. Assay of poly(3-hydroxybutyrate) depolymerase activity and product determination. Appl. Environ. Microbiol. 72(9), 6094-6100.

[23] Gheewala, S.H., Jaroenkietkajorn, U., Nilsalab, P., Silalertruksa, T., Somkerd, T., Laosiripojana, N., 2022. Sustainability assessment of palm oil-based refinery systems for food, fuel, and chemicals. Biofuel Res. J. 9(4), 1750-1763.

[24] Goswami, L., Kushwaha, A., Napathorn, S.C., Kim, B.S., 2023. Valorization of organic wastes using bioreactors for polyhydroxyalkanoate production: recent advancement, sustainable approaches, challenges, and future perspectives. Int. J. Biol. Macromol. 247, 125743.

[25] Herrmann, C., Bose, R.S., Neu, A.K., Schneider, R., Alexandri, M., 2024. Cascading valorization of defatted rice bran for lactic acid fermentation and biogas production. Biofuel Res. J. 11(3), 2146-2167.

[26] Hiroe, A., Tsuge, K., Nomura, C.T., Itaya, M., Tsuge, T., 2012. Rearrangement of gene order in the phaCAB operon leads to effective production of ultrahigh-molecular-weight poly [(R)-3-hydroxybutyrate] in genetically engineered *Escherichia coli*. Appl. Environ. Microbiol. 78(9), 3177-3184.

[27] Hiroe, A., Shiraishi, M., Mizuno, K., Tsuge, T., 2015. Behavior of different polyhydroxyalkanoate synthases in response to the ethanol level in Escherichia coli cultures. Polym. J. 47(11), 767-770.

[28] Janasch, M., Crang, N., Asplund-Samuelsson, J., Sporre, E., Bruch, M., Gynnå, A., Jahn, M., Hudson, E.P., 2022. Thermodynamic limitations of PHB production from formate and fructose in Cupriavidus necator. Metab. Eng. 73, 256-269.

[29] Jendrossek, D., Selchow, O., Hoppert, M., 2007. Poly (3-hydroxybutyrate) granules at the early stages of formation are localized close to the cytoplasmic membrane in Caryophanon latum. Appl. Environ. Microbiol. 73(2), 586-593.

[30] Jurėnas, D., Fraikin, N., Goormaghtigh, F., Van Melderen, L., 2022. Biology and evolution of bacterial toxin–antitoxin systems. Nat. Rev. Microbiol. 20(6), 335-350.

[31] Kabir, M.M., Shimizu, K., 2003a. Fermentation characteristics and protein expression patterns in a recombinant Escherichia coli mutant lacking phosphoglucose isomerase for poly(3-hydroxybutyrate) production. Appl. Microbiol. Biotechnol. 62(2-3), 244-255.

[32] Kabir, M.M., Shimizu, K., 2003b. Gene expression patterns for metabolic pathway in pgi knockout Escherichia coli with and without phb genes based on RT-PCR. J. Biotechnol. 105(1-2), 11-31.

[33] Kachrimanidou, V., Ioannidou, S.M., Ladakis, D., Papapostolou, H., Kopsahelis, N., Koutinas, A.A., Kookos, I.K., 2021. Techno-economic evaluation and life-cycle assessment of poly (3-hydroxybutyrate) production within a biorefinery concept using sunflower-based biodiesel industry by-products. Bioresour. Technol. 326, 124711.

[34] Kim, Y.E., Cho, K.H., Bang, I., Kim, C.H., Ryu, Y.S., Kim, Y., Choi, E.M., Nong, L.K., Kim, D., Lee, S.K., 2022. Characterization of an Entner-Doudoroff pathway-activated Escherichia coli. Biotechnol. Biofuels Bioprod. 15(1), 120.

[35] Koller, M., Hesse, P., Bona, R., Kutschera, C., Atlić, A., Braunegg, G., 2007. Potential of various archae- and eubacterial strains as industrial polyhydroxyalkanoate producers from whey. Macromol. Biosci. 7(2), 218-226.

[36] Kookos, I.K., Koutinas, A., Vlysidis, A., 2019. Life cycle assessment of bioprocessing schemes for poly (3-hydroxybutyrate) production

Please cite this article as: Pachimsawat J., Tsuge T., Napathorn S.C. Rewiring *Escherichia coli* central carbon metabolism for the sustainable bioconversion of waste glycerol into biodegradable polyhydroxybutyrate. Biofuel Research Journal 47 (2025) 2451-2469. DOI: 10.18331/BRJ2025.12.3.2.

using soybean oil and sucrose as carbon sources. Resour. Conserv. Recycl. 141, 317-328.
[37] Lee, H.J., Jung, H.J., Kim, B., Cho, D.H., Kim, S.H., Bhatia, S.K., Gurav, R., Kim, Y.G., Jung, S.W., Park, H.J., Yang, Y.H., 2023. Enhancement of polyhydroxybutyrate production by introduction of heterologous phasin combination in Escherichia coli. Int. J. Biol. Macromol. 225, 757-766.
[38] Lee, S.Y., Choi, J.i., 1998. Effect of fermentation performance on the economics of poly(3-hydroxybutyrate) production by Alcaligenes latus. Polym. Degrad. Stab. 59(1), 387-393.
[39] Lim, S.J., Jung, Y.M., Shin, H.D., Lee, Y.H., 2002. Amplification of the NADPH-related genes zwf and gnd for the oddball biosynthesis of PHB in an E. coli transformant harboring a cloned phbCAB operon. J. Biosci. Bioeng. 93(6), 543-549.
[40] Lin, Z., Xu, Z., Li, Y., Wang, Z., Chen, T., Zhao, X., 2014. Metabolic engineering of *Escherichia coli* for the production of riboflavin. Microb. Cell. Fact. 13, 104.
[41] Lin, Z., Zhang, Y., Yuan, Q., Liu, Q., Li, Y., Wang, Z., Ma, H., Chen, T., Zhao, X., 2015. Metabolic engineering of *Escherichia coli* for poly(3-hydroxybutyrate) production viathreonine bypass. Microb. Cell Fact. 14(1), 185.
[42] Ling, C., Qiao, G.Q., Shuai, B.W., Olavarria, K., Yin, J., Xiang, R.J., Song, K.N., Shen, Y.H., Guo, Y., Chen, G.Q., 2018. Engineering NADH/NAD+ ratio in Halomonas bluephagenesis for enhanced production of polyhydroxyalkanoates (PHA). Metabolic Eng. 49, 275-286.
[43] Long, C.P., Antoniewicz, M.R., 2019. Metabolic flux responses to deletion of 20 core enzymes reveal flexibility and limits of E. coli metabolism. Metab. Eng. 55, 249-257.
[44] Meyer, F., Keller, P., Hartl, J., Gröninger, O.G., Kiefer, P., Vorholt, J.A., 2018. Methanol-essential growth of *Escherichia coli*. Nat. Commun. 9(1), 1508.
[45] Mudliar, S.N., Vaidya, A.N., Suresh Kumar, M., Dahikar, S., Chakrabarti, T., 2008. Techno-economic evaluation of PHB production from activated sludge. Clean Technol. Environ. Policy. 10(3), 255-262.
[46] Napathorn, S.C., Visetkoop, S., Pinyakong, O., Okano, K., Honda, K., 2021. Polyhydroxybutyrate (PHB) production using an arabinose-inducible expression system in comparison with cold shock inducible expression system in Escherichia coli. Front. Bioeng. Biotechnol. 9, 661096.
[47] Ng, C.Y., Farasat, I., Maranas, C.D., Salis, H.M., 2015. Rational design of a synthetic Entner-Doudoroff pathway for improved and controllable NADPH regeneration. Metab. Eng. 29, 86-96.
[48] Olavarria, K., Pijman, Y.O., Cabrera, R., van Loosdrecht, M.C.M., Wahl, S.A., 2022. Engineering an acetoacetyl-CoA reductase from Cupriavidus necator toward NADH preference under physiological conditions. Sci. Rep. 12(1), 3757.
[49] Phithakrotchanakoon, C., Champreda, V., Aiba, S. I., Pootanakit, K., Tanapongpipat, S., 2015. Production of polyhydroxyalkanoates from crude glycerol using recombinant *Escherichia coli*. J. Polym. Environ. 23(1), 38-44.
[50] Phothong, N., Boontip, T., Chouwatat, P., Aht-Ong, D., Napathorn, S.C., 2024. Preparation and characterization of astaxanthin-loaded biodegradable polyhydroxybutyrate (PHB) microbeads for personal care and cosmetic applications. Int. J. Biol. Macromol. 257, 128709.
[51] Phothong, N., Pattarakankul, T., Morikane, S., Palaga, T., Aht-Ong, D., Honda, K., Napathorn, S.C., 2024. Stability and release mechanism of double emulsification (W1/O/W2) for biodegradable pH-responsive polyhydroxybutyrate/cellulose acetate phthalate microbeads loaded with the water-soluble bioactive compound niacinamide. Int. J. Biol. Macromol. 271(Pt 2), 132680.
[52] Rangel, C., Carvalho, G., Oehmen, A., Frison, N., Lourenco, N.D., Reis, M.A., 2023. Polyhydroxyalkanoates production from ethanol- and lactate-rich fermentate of confectionary industry effluents. Int. J. Biol. Macromol. 229, 713-723.
[53] Renouf, M., Wegener, M., Nielsen, L., 2008. An environmental life cycle assessment comparing Australian sugarcane with US corn and UK sugar beet as producers of sugars for fermentation. Biomass Bioenergy. 32(12), 1144-1155.
[54] Ritchie, G.A., Senior, P.J., Dawes, E.A., 1971. The purification and characterization of acetoacetyl-coenzyme A reductase from Azotobacter beijerinckii. Biochem. J. 121(2), 309-316.
[55] Rui, B., Shen, T., Zhou, H., Liu, J., Chen, J., Pan, X., Liu, H., Wu, J., Zheng, H., Shi, Y., 2010. A systematic investigation of Escherichia coli central carbon metabolism in response to superoxide stress. BMC Syst. Biol. 4, 122.
[56] Sanchez, A.M., Andrews, J., Hussein, I., Bennett, G.N., San, K.Y., 2006. Effect of overexpression of a soluble pyridine nucleotide transhydrogenase (UdhA) on the production of poly(3-hydroxybutyrate) in Escherichia coli. Biotechnol. Prog. 22(2), 420-425.
[57] Saratale, R.G., Cho, S.-K., Bharagava, R.N., Patel, A.K., Vivekanand, V., Bhatia, S.K., Ferreira, L.F.R., Shin, H.S., Awasthi, M.K., Chakrabortty, S., Kumar, R., Saratale, G.D., 2024. Third-generation biomass for bioplastics: a comprehensive review of microalgae-driven polyhydroxyalkanoate production. Biofuel Res. J. 11(4), 2256-2282.
[58] Sauer, U., Canonaco, F., Heri, S., Perrenoud, A., Fischer, E., 2004. The soluble and membrane-bound transhydrogenases UdhA and PntAB have divergent functions in NADPH metabolism of Escherichia coli. J. Biol. Chem. 279(8), 6613-6619.
[59] Seoane, I.T., Manfredi, L.B., Cyras, V.P., 2018. Effect of two different plasticizers on the properties of poly (3-hydroxybutyrate) binary and ternary blends. J. Appl. Polym. Sci. 135(12), 46016.
[60] Seol, E., Ainala, S.K., Sekar, B.S., Park, S., 2014. Metabolic engineering of Escherichia coli strains for co-production of hydrogen and ethanol from glucose. Int. J. Hydrogen Energy. 39(33), 19323-19330.
[61] Sheu, D.S., Chen, W.M., Lai, Y.W., Chang, R.C., 2012. Mutations derived from the thermophilic polyhydroxyalkanoate synthase PhaC enhance the thermostability and activity of PhaC from *Cupriavidus necator* H16. J. Bacteriol. 194, 2620-2629.
[62] Shimaoka, M., Kawasaki, H., Takenaka, Y., Kurahashi, O., Matsui, H., 2005. Effects of edd and pgi disruptions on inosine accumulation in Escherichia coli. Biosci. Biotechnol. Biochem. 69(7), 1248-1255.
[63] Siedler, S., Bringer, S., Blank, L.M., Bott, M., 2012. Engineering yield and rate of reductive biotransformation in *Escherichia coli* by partial cyclization of the pentose phosphate pathway and PTS-independent glucose transport. Appl. Microbiol. Biotechnol. 93(4), 1459-1467.
[64] Sikazwe, M.K., Louw, J., Görgens, J.F., 2024. Techno-economic and environmental assessment of a sugarcane biorefinery: direct and indirect production pathways of biobased adipic acid. Biofuel Res. J. 11(4), 2225-2242.
[65] Sim, S., Snell, K., Kim, B., Rha, C., Sinskey, A., 2001. Increased poly-β-hydroxybutyrate (PHB) chain length by the modulation of PHA synthase activity in recombinant Escherichia coli. Biotechnol. Lett. 23, 2057-2061.
[66] Simonzadeh, N., Ronsen, B., 2012. An isocratic HPLC method for the determination of sorbitol and glycerol in pharmaceutical formulations. J. Chromatogr. Sci. 50(7), 644-647.
[67] Sinsukudomchai, P., Aht-Ong, D., Honda, K., Napathorn, S.C., 2023. Green composites made of polyhydroxybutyrate and long-chain fatty acid esterified microcrystalline cellulose from pineapple leaf. Plos one. 18(3), e0282311.
[68] Škulj, M., Okršlar, V., Jalen, Š., Jevševar, S., Slanc, P., Štrukelj, B., Menart, V., 2008. Improved determination of plasmid copy number using quantitative real-time PCR for monitoring fermentation processes. Microb. Cell Fact. 7(1), 6.
[69] Stincone, A., Prigione, A., Cramer, T., Wamelink, M.M., Campbell, K., Cheung, E., Olin-Sandoval, V., Grüning, N.M., Krüger, A., Tauqeer Alam, M., 2015. The return of metabolism: biochemistry and physiology of the pentose phosphate pathway. Biol. Rev. 90(3), 927-963.
[70] Sun, S., Ding, Y., Liu, M., Xian, M., Zhao, G., 2020. Comparison of glucose, acetate and ethanol as carbon resource for production of poly(3-Hydroxybutyrate) and other acetyl-CoA derivatives. Front. Bioeng. Biotechnol. 8, 833.
[71] Suresh, S., Naik, A., Premanath, R., 2023. Glucose-induced enhanced virulence in strains of multidrug-resistant Pseudomonas aeruginosa isolated from diabetic patients. Curr. Microbiol. 80(3), 100.

Please cite this article as: Pachimsawat J., Tsuge T., Napathorn S.C. Rewiring *Escherichia coli* central carbon metabolism for the sustainable bioconversion of waste glycerol into biodegradable polyhydroxybutyrate. Biofuel Research Journal 47 (2025) 2451-2469. DOI: 10.18331/BRJ2025.12.3.2.

[72] Tian, J., Sinskey, A.J., Stubbe, J., 2005. Kinetic studies of polyhydroxybutyrate granule formation in Wautersia eutropha H16 by transmission electron microscopy. J. Bacteriol. 187(11), 3814-3824.
[73] Tsuge, T., 2016. Fundamental factors determining the molecular weight of polyhydroxyalkanoate during biosynthesis. Polym. J. 48(11), 1051-1057.
[74] Tyo, K.E., Ajikumar, P.K., Stephanopoulos, G., 2009. Stabilized gene duplication enables long-term selection-free heterologous pathway expression. Nat. Biotechnol. 27(8), 760-765.
[75] Vasiljevs, S., Gupta, A., Baines, D., 2023. Effect of glucose on growth and co-culture of Staphylococcus aureus and Pseudomonas aeruginosa in artificial sputum medium. Heliyon. 9(11), e21469.
[76] Wei, J., Li, Y., 2023. CRISPR-based gene editing technology and its application in microbial engineering. Eng. Microbiol. 3(4), 100101.
[77] Wongmoon, C., Napathorn, S.C., 2022. Optimization for the efficient recovery of poly (3-hydroxybutyrate) using the green solvent 1, 3-dioxolane. Front. Bioeng. Biotechnol. 10.
[78] Wu, H., Wang, H., Chen, J., Chen, G.Q., 2014. Effects of cascaded vgb promoters on poly (hydroxybutyrate)(PHB) synthesis by recombinant *Escherichia coli* grown micro-aerobically. Appl. Microbiol. Biotechnol. 98(24), 10013-10021.
[79] Wu, H., Chen, J., Chen, G.-Q., 2016. Engineering the growth pattern and cell morphology for enhanced PHB production by Escherichia coli. Appl. Microbiol. Biotechnol. 100(23), 9907-9916.
[80] Wu, H., Li, S., Ji, M., Chen, Q., Shi, J., Blamey, J.M., Sun, J., 2020. Improvement of polyhydroxybutyrate production by deletion of csrA in Escherichia coli. Electron. J. Biotechnol. 46, 8-13.
[81] Xiong, B., Yang, T., Zhang, Z., Li, X., Yu, H., Wang, L., You, Z., Peng, W., Jin, L., Song, H., 2025. Metabolic reprogramming and machine learning-guided cofactor engineering to boost nicotinamide mononucleotide production in Escherichia coli. Bioresour. Technol. 426, 132350.
[82] Zhang, Z., Gosset, G., Barabote, R., Gonzalez, C.S., Cuevas, W.A., Saier, M.H., Jr., 2005. Functional interactions between the carbon and iron utilization regulators, Crp and Fur, in Escherichia coli. J. Bacteriol. 187(3), 980-990.
[83] Zhao, X., Xu, J., Tan, M., Zhen, J., Shu, W., Yang, S., Ma, Y., Zheng, H., Song, H., 2020. High copy number and highly stable Escherichia coli-Bacillus subtilis shuttle plasmids based on pWB980. Microb. Cell Fact. 19, 1-12.

Ms. Jittakan Pachimsawat is currently a Ph.D. candidate in the Biotechnology Program at the Faculty of Science, Chulalongkorn University, Thailand. She obtained her Bachelor of Science degree with second-class honors in biochemistry from the Faculty of Science, Chulalongkorn University, and subsequently entered the university's integrated M.Sc.–Ph.D. program. Her research interests focus on genetic engineering, microbial strain improvement, and the biosynthesis of polyhydroxyalkanoates. ORCID: 0009-0005-9101-0056.

Takeharu Tsuge, Ph.D., is a Professor in the Department of Materials Science and Engineering, Institute of Science, Tokyo, Japan. He received his doctoral degree in agriculture (applied microbiology) from Kyushu University, Japan, in 2000. He joined the Polymer Chemistry Laboratory at RIKEN as a Special Postdoctoral Researcher (2000–2002) and at Tokyo Institute of Technology as an Assistant Professor (2002–2005). He was promoted to an Associate Professor in 2009 and a Professor in 2024. In October 2024, the Tokyo Institute of Technology was reorganized as the Institute of Science Tokyo. He received the Encouragement Award (Terui Award) from the Society for Biotechnology, Japan (2008) and the SPSJ Asahi Kasei Award from the Society of Polymer Science, Japan (2015). His current research interests include microbial polyester synthesis and biobased polymeric materials. He has published 172 ISI/Scopus-indexed papers and has an h-index of 36, with over 4,700 citations. ORCID: 0000-0002-6296-6500 | Scopus ID: 7006827234.

Suchada Chanprateep Napathorn, Ph.D., is an Associate Professor in the Department of Microbiology, Faculty of Science, Chulalongkorn University, Thailand. She received her Ph.D. in biotechnology engineering from the University of Osaka, Japan, in 2002 and completed a postdoctoral fellowship at the Cornell/Ludwig Institute for Cancer Research, USA, in 2005. She received the Excellent Paper Award from The Society for Biotechnology, Japan (2007), the Young Asian Biotechnologist Prize from The Society for Biotechnology, Japan (2009), the Outstanding Young Scientist Award from the Faculty of Science, Chulalongkorn University, Thailand (2010), and the NRCT Quality Achievement Award from the National Research Council of Thailand (NRCT) (2025). She served as a Specially Appointed Associate Professor (2019–2024) and is currently a Visiting Researcher (2024–2026) at the International Center for Biotechnology, University of Osaka, Japan. Her research focuses on bioprocess systems and microbial biotechnology, particularly the production and application of biodegradable polyhydroxyalkanoates (PHAs), bioprocess development, and waste valorization. She has published 39 ISI/Scopus-indexed papers, authored four textbooks, and filed six patent/petty patent applications. She has an h-index of 16, with over 1,200 citations, and was listed among the world's top 2% of scientists by Elsevier/Stanford University in 2022 and 2024. ORCID: 0000-0002-3598-9344 | Scopus ID: 15519013300.

Please cite this article as: Pachimsawat J., Tsuge T., Napathorn S.C. Rewiring *Escherichia coli* central carbon metabolism for the sustainable bioconversion of waste glycerol into biodegradable polyhydroxybutyrate. Biofuel Research Journal 47 (2025) 2451-2469. DOI: 10.18331/BRJ2025.12.3.2.

Supplementary Information

Table S1.
Time courses of PHB production by recombinant E. coli Δedd-pBSK-CAB$_{A-04}$, Δpgi-pBSK-CAB$_{A-04}$ and K12-pBSK-CAB$_{A-04}$ in LB medium supplemented with 20 g/L glucose as the sole carbon source in flask scale at 30 °C for 48 h.

Time (h)	CDM (g/L)	PHB (g/L)	RCM (g/L)	PHB content (wt%)	Glucose (g/L)	Productivity (g/L·h)
Δ*edd*-pBSK-*CAB*$_{A-04}$						
6	0.7 ± 0.1	0.1 ± 0.0	0.6 ± 0.1	16.3 ± 1.9	19.2 ± 0.5	0.02
12	3.2 ± 0.2	2.5 ± 0.2	0.8 ± 0.2	76.5 ± 1.8	16.0 ± 0.6	0.21
24	7.5 ± 0.5	6.8 ± 0.2	0.7 ± 0.5	91.2 ± 5.2	6.6 ± 0.4	0.28
30	8.1 ± 0.4	7.6 ± 0.4	0.6 ± 0.3	93.0 ± 2.3	4.0 ± 0.5	0.25
36	7.8 ± 0.6	6.8 ± 0.7	1.0 ± 0.3	86.9 ± 3.5	0	0.19
48	9.3 ± 0.5	7.6 ± 0.5	1.8 ± 0.5	81.1 ± 0.5	0	0.16
Δ*pgi*-pBSK-*CAB*$_{A-04}$						
6	0.5 ± 0.3	0.0 ± 0.0	0.4 ± 0.1	4.2 ± 1.3	20.5 ± 0.0	0.00
12	2.5 ± 0.5	0.6 ± 0.1	1.9 ± 0.5	25.6 ± 2.2	17.9 ± 0.6	0.05
24	5.7 ± 0.4	3.1 ± 0.2	2.0 ± 0.2	60.3 ± 3.2	7.5 ± 1.2	0.13
30	6.5 ± 0.5	4.5 ± 0.5	2.0 ± 0.4	69.2 ± 3.9	4.1 ± 0.1	0.15
36	7.6 ± 0.7	5.1 ± 0.6	2.5 ± 0.7	66.9 ± 3.4	0	0.14
48	7.8 ± 0.5	5.7 ± 0.5	2.2 ± 0.4	72.4 ± 2.7	0	0.12
K12-pBSK-*CAB*$_{A-04}$						
6	1.8 ± 0.4	0.2 ± 0.1	1.7 ± 0.3	9.6 ± 2.0	21.5 ± 1.3	0.03
12	5.5 ± 0.2	3.5 ± 0.1	1.9 ± 0.2	65.0 ± 0.9	15.9 ± 0.6	0.30
24	6.9 ± 0.4	5.0 ± 0.4	1.8 ± 0.3	73.5 ± 2.8	10.5 ± 0.6	0.21
30	9.7 ± 0.5	7.1 ± 0.7	2.6 ± 0.3	73.1 ± 6.2	4.3 ± 0.2	0.24
36	9.6 ± 0.7	7.1 ± 1.1	2.6 ± 0.6	73.2 ± 8.6	4.1 ± 0.1	0.20
48	9.6 ± 0.8	7.3 ± 0.4	2.3 ± 0.8	76.5 ± 2.9	0	0.15

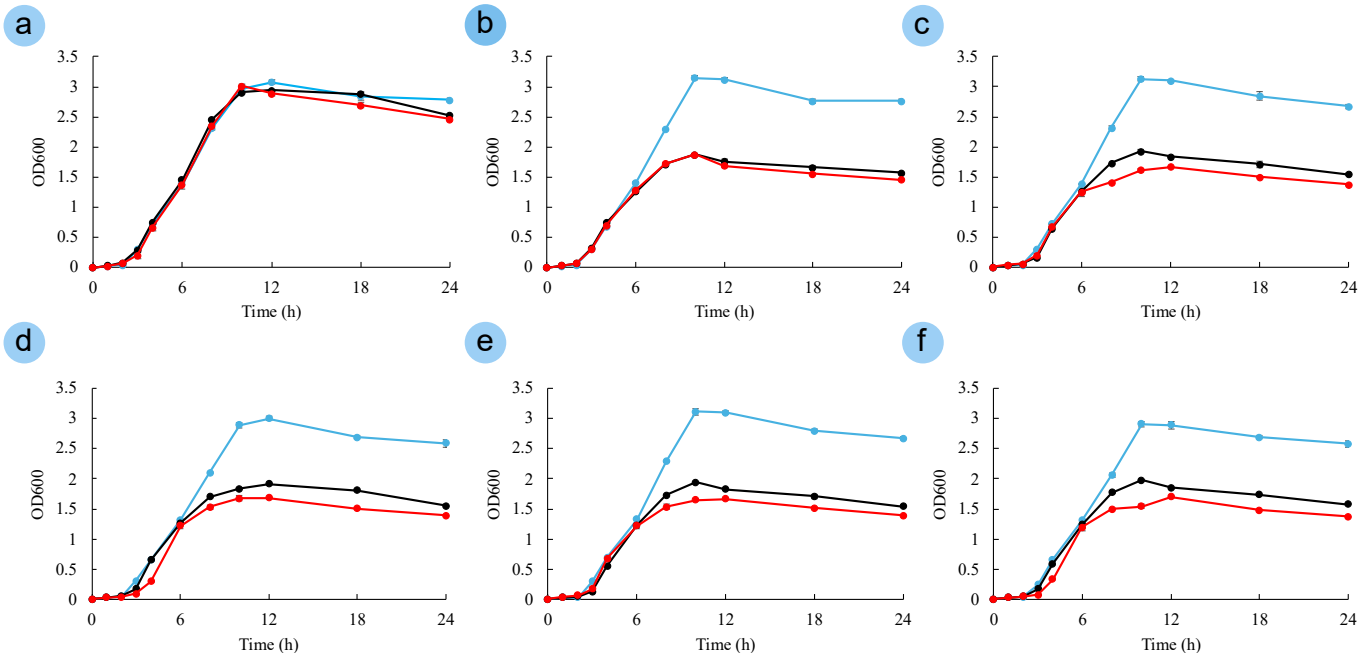

Fig. S1. Bacterial growth of *E. coli* strain K12, Δ*pgi* and Δ*edd* on different concentration of glucose, 0 g/L **(a)**, 2.5 g/L **(b)**, 5 g/L **(c)**, 10 g/L **(d)**, 15 g/L **(e)**, and 20 g/L **(f)** (n = 3) over a 24-h period.

Please cite this article as: Pachimsawat J., Tsuge T., Napathorn S.C. Rewiring *Escherichia coli* central carbon metabolism for the sustainable bioconversion of waste glycerol into biodegradable polyhydroxybutyrate. Biofuel Research Journal 47 (2025) 2451-2469. DOI: 10.18331/BRJ2025.12.3.2.